MODAL-REDUCTION FORMULATION USING LOCAL EIGENVALUE MODIFICATION PROCEDURE FOR HIGH-RATE APPLICATION

Emmanuel A. Ogunniyi
PhD. Candidate
Department of Mechanical Engineering, University of South Carolina, Columbia, USA
03/26/2025
Doctoral defense

Advisor: Dr. Austin R.J Downey

UNIVERSITY OF SOUTH CAROLINA

Contents

Contents

Contributions

Algorithmic Innovation: LEMP reformulated with divide-and-conquer techniques, modal reduction, and Bayesian sampling to achieve millisecond to microsecond update speeds.

$$\frac{1}{\alpha_k} = \sum_{i=1}^{m} \frac{\left(\left\{u^{(i)}\right\}^T \left\{t_k\right\}\right)^2}{\Omega_2^2 - \omega_i^2}$$

$$\frac{1}{\Omega^2 \alpha_m} = \sum_{i=1}^{m} \frac{\left(\left\{u^{(i)}\right\}^T \left\{t_m\right\}\right)^2}{\Omega_2^2 - \omega_i^2}$$

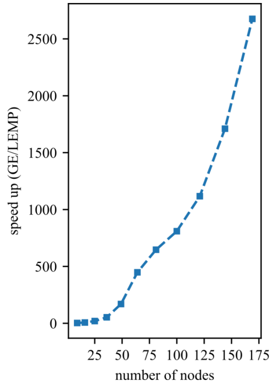

Experimental Validation: Demonstrated on real systems (DROPBEAR), showing both performance and real-time viability.

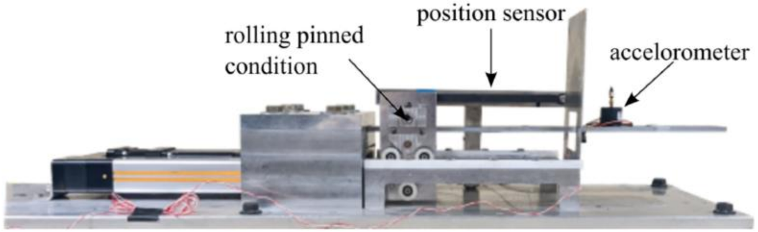

Cross-domain Applicability: Used on 1D beams, 2D plates, and PCBs — covering a broad spectrum from aerospace structures to electronics.

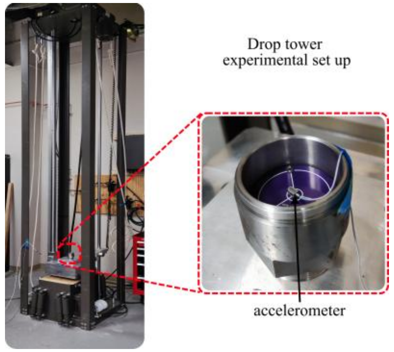

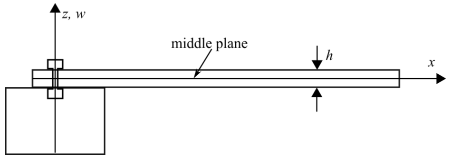

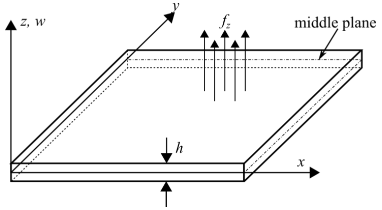

Edge-readiness: Proven to run on hardware-in-the-loop systems, ready for embedded and cyber-physical applications.

Publications towards Dissertation

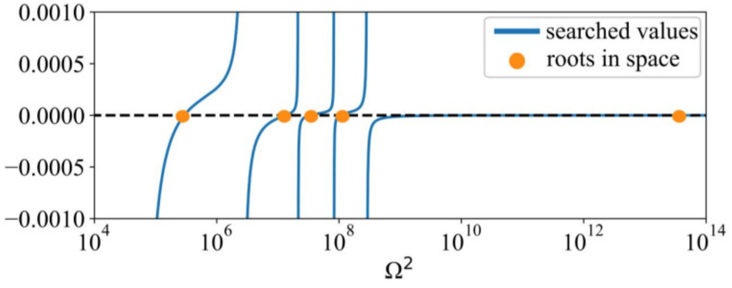

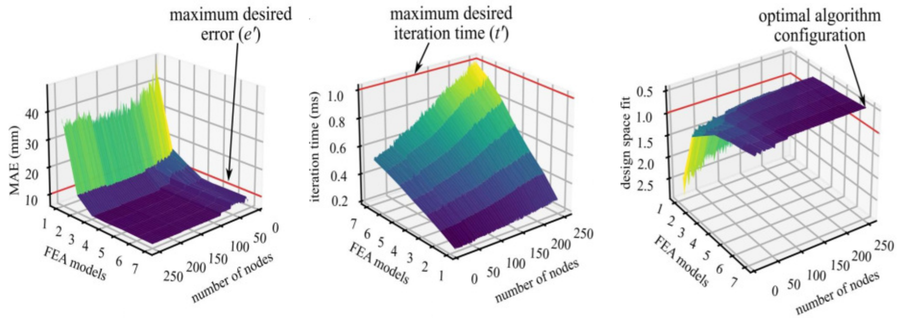

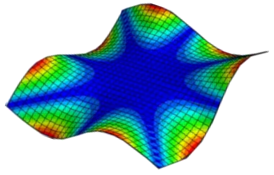

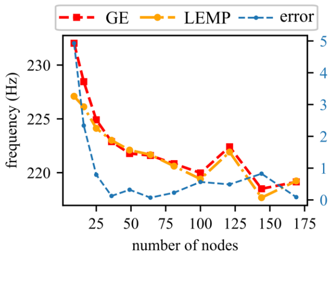

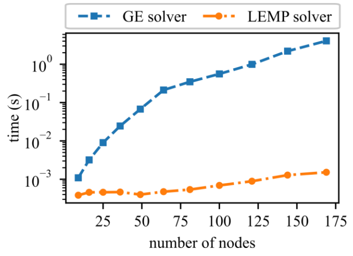

Real-time solver formulation

1. **Emmanuel A Ogunniyi**., Austin RJ Downey Jr, and Jason D. Bakos. "Development of a real-time solver for the local eigenvalue modification procedure." Sensors and Smart Structures Technologies for Civil, Mechanical, and Aerospace Systems 2022. Vol. 12046. SPIE, 2022.

1D Application (DROPBEAR Testbed)

2. **Emmanuel A Ogunniyi**, Claire Drnek, Seong Hyeon Hong, Austin RJ Downey, Yi Wang, Jason D Bakos, Peter Avitabile, and Jacob Dodson. Real-time structural model updating using local eigenvalue modification procedure for applications in high-rate dynamic events. Mechanical Systems and Signal Processing, 195:110318, 2023.

3. Vereen AB, **Ogunniyi EA**, Downey AR, Dodson J, Moura AG, Bakos JD. Online Implementation of the Local Eigenvalue Modification Procedure for High-Rate Model Assimilation. In Society for Experimental Mechanics Annual Conference and Exposition 2023 Jun 5 (pp. 121-127). Cham: Springer Nature Switzerland.

4. Vereen AB, **Ogunniyi EA**, Downey AR, Blasch E, Bakos JD, Dodson J. Optimal Sampling Methodologies for High-rate Structural Twinning. In 2023 26th International Conference on Information Fusion (FUSION) 2023 Jun 27 (pp. 1-8). IEEE.

2D Modal-formulation & Implementation

5. **Emmanuel A Ogunniyi**, Alexander B Vereen, and Austin RJ Downey. Microsecond model updating for 2d structural systems using the local eigenvalue modification procedure. Structural Health Monitoring Iwshm 2023, 2023

6. **Emmanuel O.**, Joud Satme, and Austin RJ Downey. Online model-based structural damage detection in electronic assemblies. Sensors and Smart Structures Technologies for Civil, Mechanical, and Aerospace Systems SPIE, 2024

Other Publications during Doctoral program

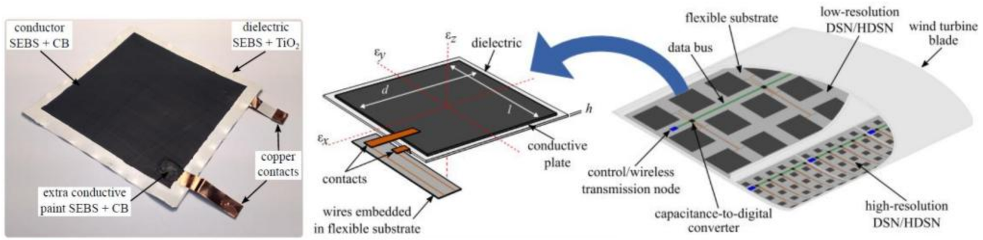

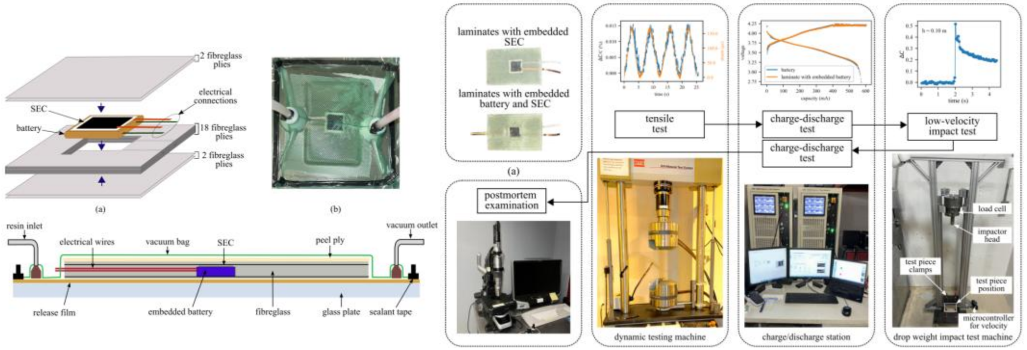

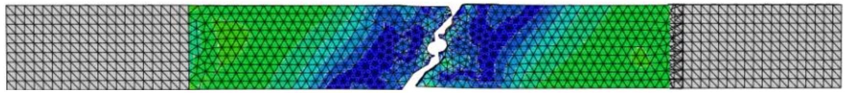

Flexible electronics (Soft Elastomeric Capacitors) - Master's thesis

1. **Emmanuel A Ogunniyi**, Han Liu, Austin RJ Downey, Simon Laflamme, Jian Li, Caroline Bennett, William Collins, Hongki Jo, and Paul Ziehl. Soft elastomeric capacitors with an extended polymer matrix for strain sensing on concrete. In 92 Sensors and Smart Structures Technologies for Civil, Mechanical, and Aerospace Systems 2023, volume 12486, pages 262270. SPIE, 2023

2. **Emmanuel Ogunniyi**, Alexander Vereen, Austin R.J. Downey, Simon Laflamme, Jian Li, Caroline R Bennett, William Collins, Hongki Jo, Alexander Henderson, and Paul Ziehl. Investigation of electrically isolated capacitive sensing skins on concrete to reduce structure/sensor capacitive coupling. Measurement Science and Technology, feb 2023. doi:10.1088/1361-6501/acbb97

3. **Emmanuel A Ogunniyi**, White John, Han Liu, Austin RJ Downey, Simon Laflamme, Jian Li, Caroline Bennett, William Collins, Hongki Jo, and Paul Ziehl. Performance evaluation of flexible capacitive sensors on non-uniform surfaces. Sensors and Smart Structures Technologies for Civil, Mechanical, and Aerospace Systems SPIE, 2024

4. **Emmanuel Ogunniyi**, Han Liu, Austin Downey, Simon Laflamme, Jian Li, Caroline R Bennett, William Collins, Hongki Jo, and Paul Ziehl. In situ assembly enabling adhesive free bonding of large area electronic sensors to concrete for structural health monitoring. *Smart Materials and Structures*, September 2024. doi:10.1088/1361-665x/ad7d56

Structural Batteries

5. Anthony George, Madden Connor, **Ogunniyi Emmanuel**, Downey Austin R.J., Limbaugh Ryan, Peskar Jarrett, Baoa Jingjing, and Xinyu Huanga. Exploratory investigation of early detection for high-c discharge-induced failure in 18650 lithium-ion batteries. Sensors and Smart Structures Technologies for Civil, Mechanical, and Aerospace Systems SPIE, 2024

6. **Emmanuel Ogunniyi**. and Downey, Austin R.J. and Sockalingam, Subramani and Liu, Han and Laflamme, Simon, Impact monitoring of embedded batteries in sandwich composites with integrated soft elastomeric capacitors, Sensors and Smart Structures Technologies for Civil, Mechanical, and Aerospace Systems SPIE 2025

7. **Emmanuel Ogunniyi**. and Downey, Austin R.J. and Sockalingam, Subramani and Liu, Han and Laflamme, Simon, In Situ Monitoring of Impact-Induced Capacity Loss in Structural Batteries with Flexible Electronics (In review)

Addictive manufacturing

8. Yanzhou Fu, Austin R.J. Downey, Lang Yuan, Hung-Tien Huang, and **Emmanuel A. Ogunniyi**. Simulation-in-the-loop additive manufacturing for real-time structural validation and digital twin development. Additive Manufacturing, 98:104631, January 2025. doi:10.1016/j.addma.2024.104631

Contents

High-rate Dynamics in the Real-world

Civil Structures Exposed to blast

Samali, B., et al., *Review of the basics of state of the art of blast loading. Asian Journal of Civil Engineering.* (2018).

High-rate Dynamics in the Real-world

Automotive safety systems against Collision

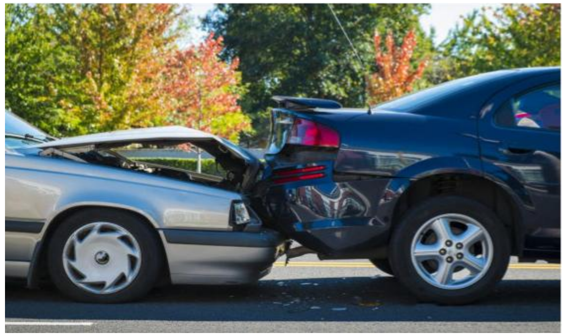

Airbag deployment

Space shuttle and Aerial Vehicles Prone to In-Flight Anomalies

Hypersonic vehicles

Ballistic packages

Lightning strikes on aircraft

Fighter jets

Description of High-rate Dynamics

High-rate (<100ms)

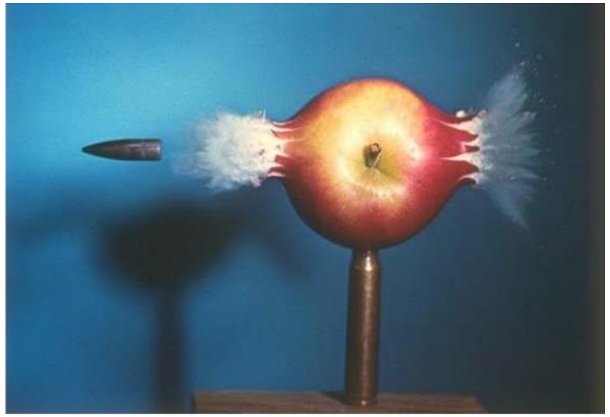

High-amplitude (acceleration > 100 *g*)

The deceleration event in drop tower tests typically lasts for 0.2ms

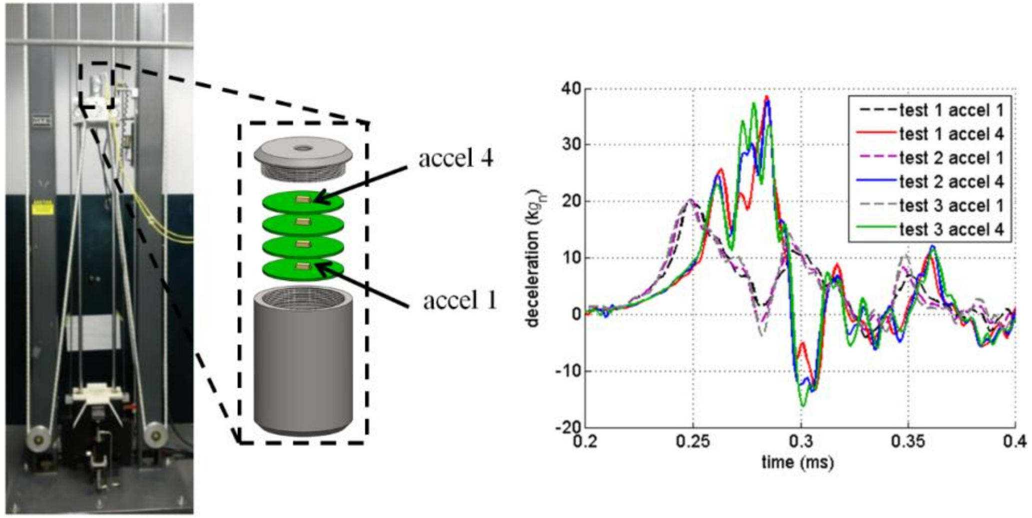

- Large uncertainties in the external loads.
- High levels of non-stationarity and heavy disturbance.
- Generations of unmodeled dynamics from changes in mechanical configuration.

GitHub

Hong, J. et al,. *Introduction to state estimation of high-rate system dynamics*. Sensors, 18(2):217, Jan 2018

Contents

Technical Challenges of Estimating State of High-rate Dynamic system

Adequate sensing

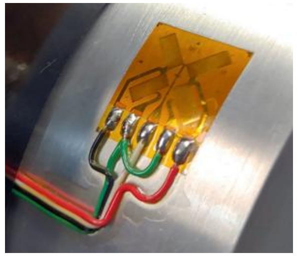

Sensor response

3 µs – 10 µs

Lack of system Knowledge

Duration of event

30 µs – 100 ms

High variability in loading

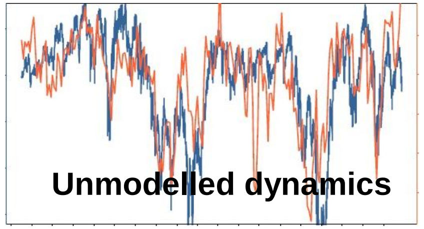

Different behavior regimes

250 µs – 1 secs

Limited resources for algorithm implementation

Algorithm execution and decision making

Main Objective

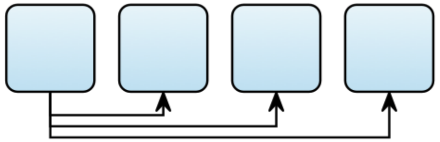

100µs-1ms

Dodson, Jacob, et al. "High-rate structural health monitoring and prognostics: an overview." *Data Science in Engineering, Volume 9* (2021): 213-217.

Methodologies for high-rate state estimation

- Physics-enhanced machine learning (PEML) models
- Real-time fusion of high-speed dynamic data augmented by model-based data
  - ✓ Model reduction and model-updating (offline and real-time) approaches
    - ❖ Finite Element model updating
- Uncertainty quantification (UQ) methods to enable decisions connected to confidences

Dodson, Jacob, et al. "High-rate structural health monitoring and prognostics: an overview." *Data Science in Engineering, Volume 9* (2021): 213-217.

Real-time FEA model updating (1D)

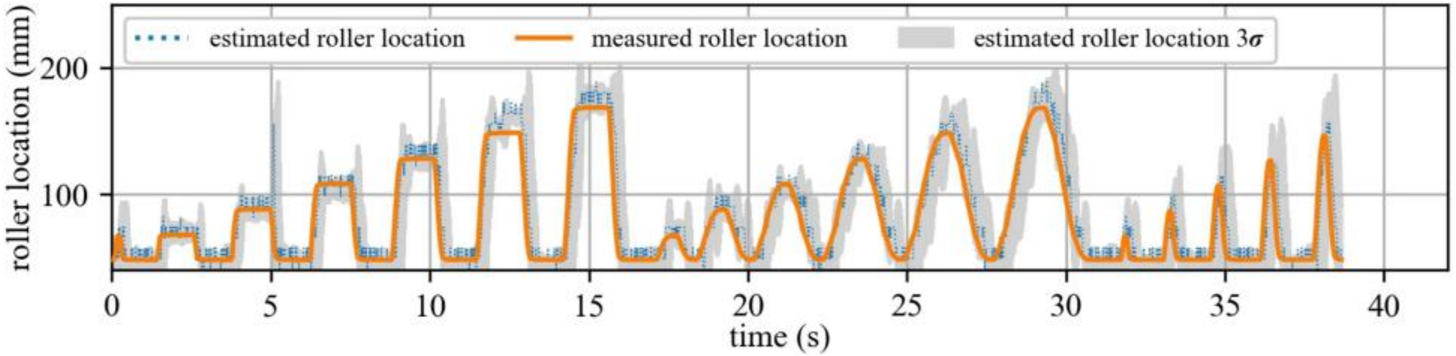

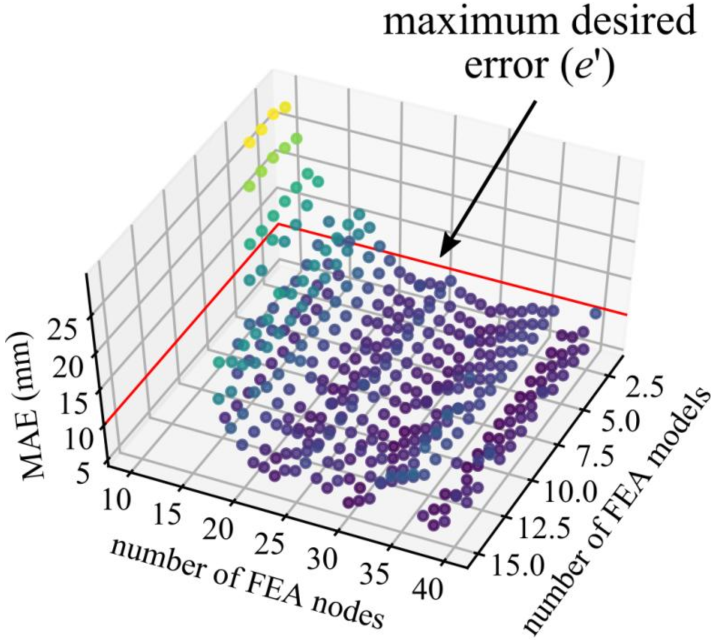

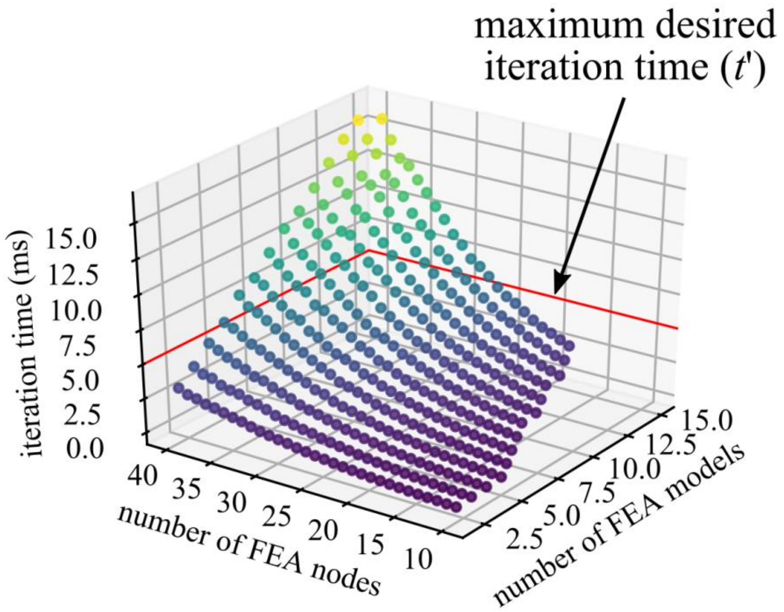

Downey A., et al,. “Millisecond Model Updating for Structures Experiencing Unmodeled High-Rate Dynamic Events” *Mechanical Systems and Signal Processing* ***138***, 2020

FEA Computation speed for the DROPBEAR

General Eigenvalue solutions accurately estimates the state of the DROPBEAR

However, FEA model is limited to 23 nodes to achieve 1ms model updating time

Solving for system's frequencies accounted for 90% of algorithm iteration time

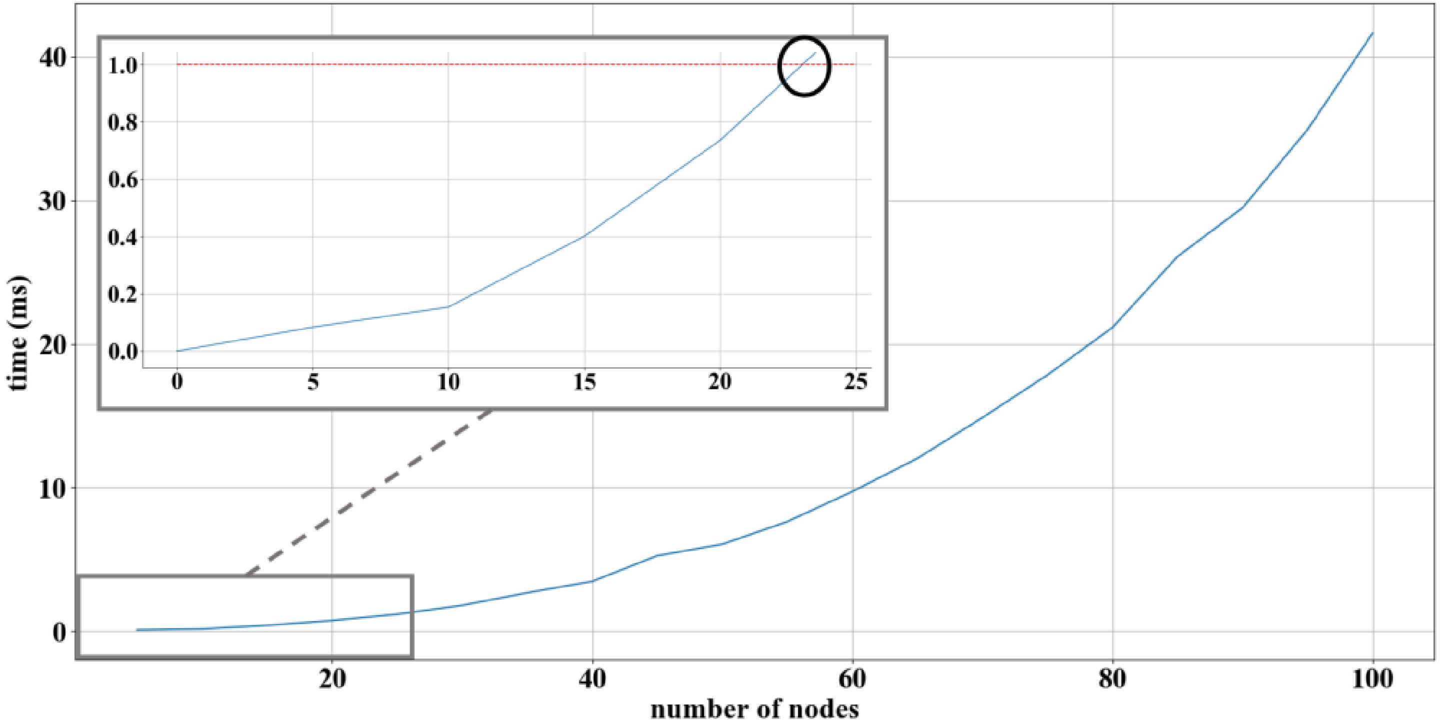

Carroll, M., Downey, A., Dodson, J., Hong, J. and Scheppegrell, J., "Analysis of Computation Speeds of Eigenvalue Solutions for High-Rate Structural Health Monitoring."

Contents

Structural Dynamic Modification

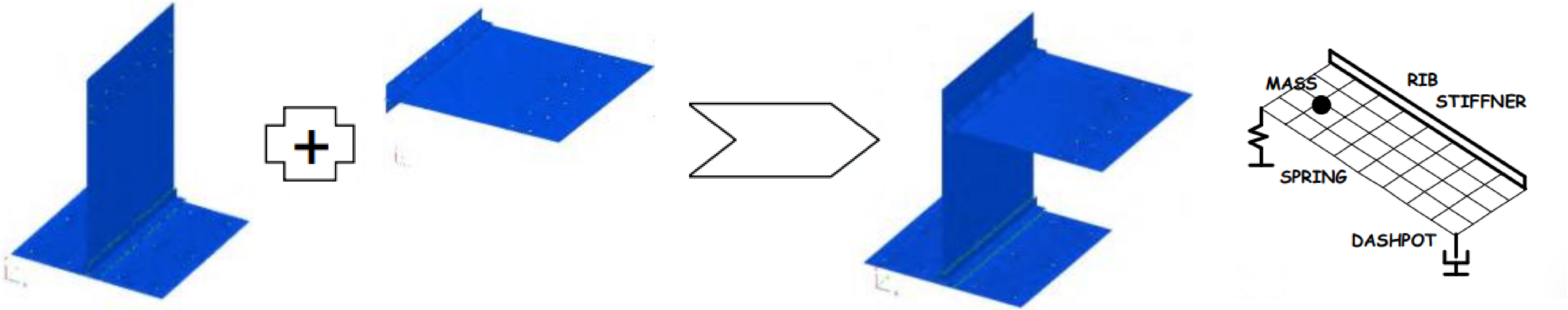

Avitabile, P., “*Twenty Years of Structural Dynamic Modification- A Review*,” *Sound and Vibration,* pp. 14-25. 2003

Eigenvalue Modification Procedure

Can the existing frequencies and mode shapes be used to predict new frequencies and mode shapes dues to changes in mass and stiffness?

$$\left[\begin{bmatrix}\ddots & & \\ & \overline{M}_1 & \\ & & \ddots\end{bmatrix}+\left[\Delta\overline{M}_{12}\right]\right]\{\ddot{p}_1\}+\left[\begin{bmatrix}\ddots & & \\ & \overline{K}_1 & \\ & & \ddots\end{bmatrix}+\left[\Delta\overline{K}_{12}\right]\right]\{p_1\}=[0]$$

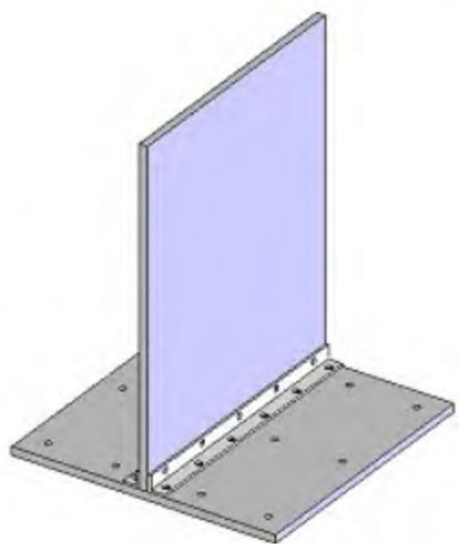

$$\left[\Delta\overline{M}_{12}\right]=[U_1]^T[\Delta M_{12}][U_1]$$

$$\left[\Delta\overline{K}_{12}\right]=[U_1]^T[\Delta K_{12}][U_1]$$

$$\left[\left[\begin{bmatrix}\ddots & & \\ & \overline{K}_1 & \\ & & \ddots\end{bmatrix}+[U_1]^T[\Delta K_{12}][U_1]\right]-\lambda\left[\begin{bmatrix}\ddots & & \\ & \overline{M}_1 & \\ & & \ddots\end{bmatrix}+[U_1]^T[\Delta M_{12}][U_1]\right]\right]\{p_1\}=\{0\}$$

Avitabile, P., “*Twenty Years of Structural Dynamic Modification- A Review*,” *Sound and Vibration,* pp. 14-25. 2003

Local Eigenvalue Modification Procedure (LEMP)

What is LEMP?

- Identifies physical changes to the system such as mass, stiffness or damping representing them in terms of frequencies or mode shapes
- Model the altered state as a mixture of the initial state and changes made to the initial state
- Reduces the GE equation to a set of second-order equations

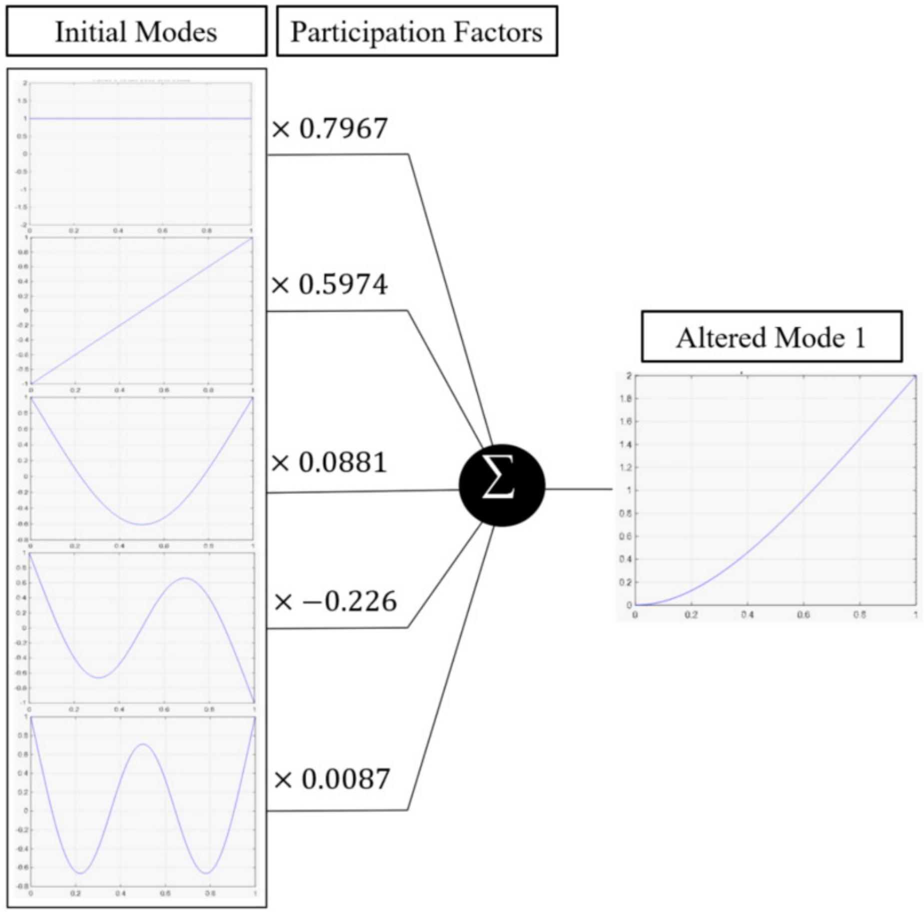

Avitabile, P., "*Twenty Years of Structural Dynamic Modification- A Review*," *Sound and Vibration,* pp. 14-25. 2003

Local Eigenvalue Modification Procedure (LEMP)

If only one change of mass or stiffness is considered, then this equations can be reduced to

Stiffness change

$$\left[\left[\begin{bmatrix}\ddots & & \\ & \overline{K}_1 & \\ & & \ddots\end{bmatrix} + \{v_{1k}\}\alpha_{1k}\{v_{1k}\}^T\right] - \lambda\left[\begin{bmatrix}\ddots & & \\ & \overline{M}_1 & \\ & & \ddots\end{bmatrix}\right]\right]\{p_1\} = \{0\}$$

Mass change

$$\left[\left[\begin{bmatrix}\ddots & & \\ & \overline{K}_1 & \\ & & \ddots\end{bmatrix}\right] - \lambda\left[\begin{bmatrix}\ddots & & \\ & \overline{M}_1 & \\ & & \ddots\end{bmatrix} + \{v_{1m}\}\alpha_{1m}\{v_{1m}\}^T\right]\right]\{p_1\} = \{0\}$$

The solution then reduces to a second order equation for each of the ‘m’ modes of the system

A solver for the equation was formulated using Divide and Conquer method

$$\frac{1}{\alpha_k} = \sum_{i=1}^{m} \frac{\left(\left\{u^{(i)}\right\}^T \{t_k\}\right)^2}{\Omega_2^2 - \omega_i^2}$$

$$\frac{1}{\Omega^2 \alpha_m} = \sum_{i=1}^{m} \frac{\left(\left\{u^{(i)}\right\}^T \{t_m\}\right)^2}{\Omega_2^2 - \omega_i^2}$$

Avitabile, P., “*Twenty Years of Structural Dynamic Modification- A Review*,” *Sound and Vibration,* pp. 14-25. 2003

Single-State change Estimation

- Initial state general eigenvalue solution

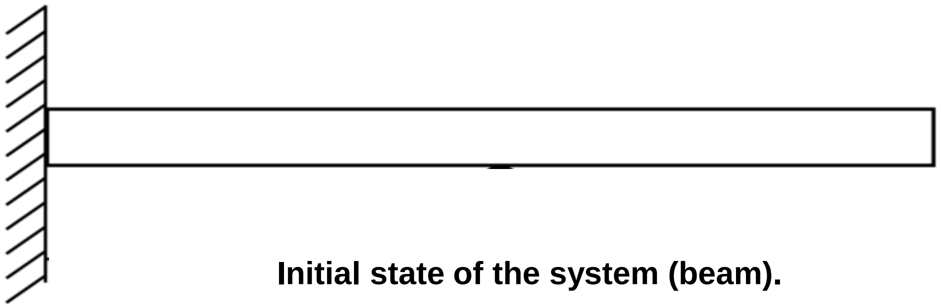

Initial state of the system (beam).

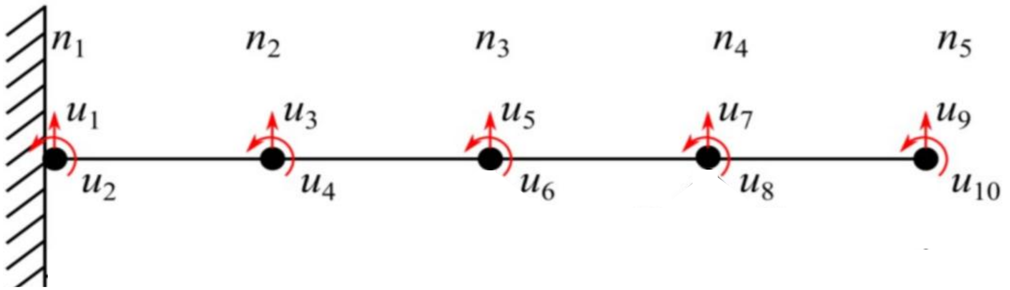

$$\boldsymbol{\lambda} = (60237 \quad 2682286 \quad 21391038 \quad 82438554 \quad 286161582)$$

Construct the elemental mass and stiffness matrices ($\mathbf{M}_1$ and $\mathbf{K}_1$)

Solve the general eigenvalue problem to obtain the squares of the first n natural frequencies, and the first n modal vectors for the initial state

$$\mathbf{U}_1 = \begin{pmatrix} -0.000005 & 0.00011 & 0.00051 & 0.00138 & -0.00340 \\ -0.000001 & 0.000008 & 0.000023 & 0.000046 & -0.000088 \\ -0.184749 & 0.862567 & 1.521322 & 1.535297 & -0.796654 \\ -3.95962 & 13.68743 & 10.37102 & -17.27622 & 68.83187 \\ -0.64779 & 1.52565 & 0.15321 & -1.53923 & 0.260667 \\ -6.37642 & -1.72852 & -3.28287 & -6.21277 & -80.17702 \\ -1.26088 & 0.420824 & -1.25908 & 1.14986 & 0.176068 \\ -7.43893 & -2.20332 & 13.1159 & 21.2392 & 76.3001 \\ -1.92314 & -1.86050 & 1.94283 & -1.87065 & -1.9711 \\ -7.61313 & -27.5937 & 46.6347 & -63.1058 & -96.1961 \end{pmatrix}$$

$$f_1 = (39 \quad 261 \quad 736 \quad 1445 \quad 2692)$$

LEMP Implementation

- **Step 1: Addition of roller condition (change)**

$$\Delta\mathbf{K}_{12} = (0 \quad 0 \quad 0 \quad 0 \quad 0 \quad 0 \quad 0 \quad 1e10 \quad 0 \quad 0)$$

- **Step 2: Spectral decomposition of $\Delta\mathbf{K}_{12}$**

$$\mathrm{T} = (1 \quad 1 \quad 1 \quad 1 \quad 1 \quad 1 \quad 1 \quad 1 \quad 1 \quad 1)$$

$$\alpha = (0 \quad 0 \quad 0 \quad 0 \quad 0 \quad 0 \quad 0 \quad 1e10 \quad 0 \quad 0)$$

- **Step 3: Set truncation: include only contributing modes**

The contributing vectors are reduced to only those values in the 8th row of each matrix.

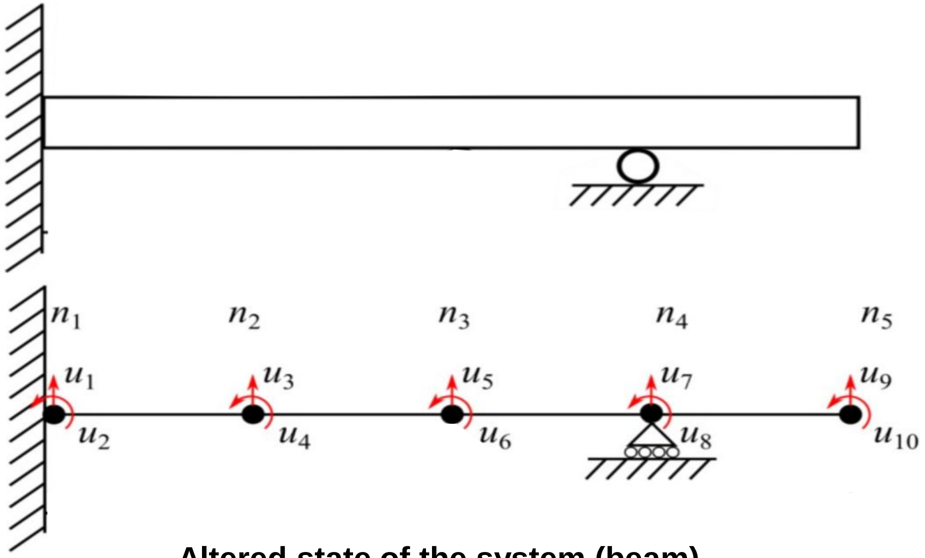

Altered state of the system (beam) with added roller condition (spring)

LEMP Implementation

- **Step 4: Obtain Ω^2 using Divide and conquer**

Ω^2 values using D&C and Sympy function “solveset”

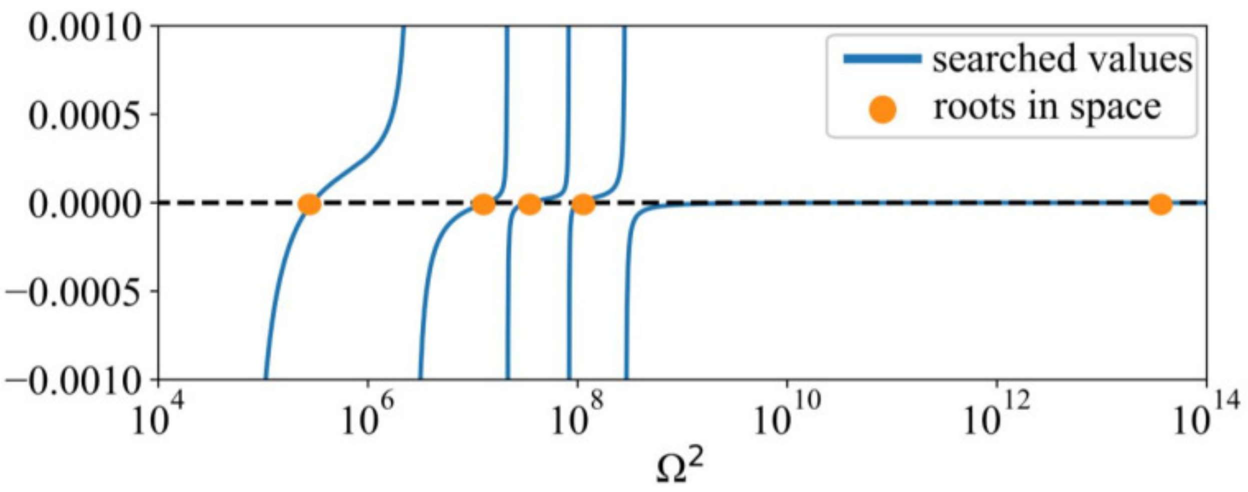

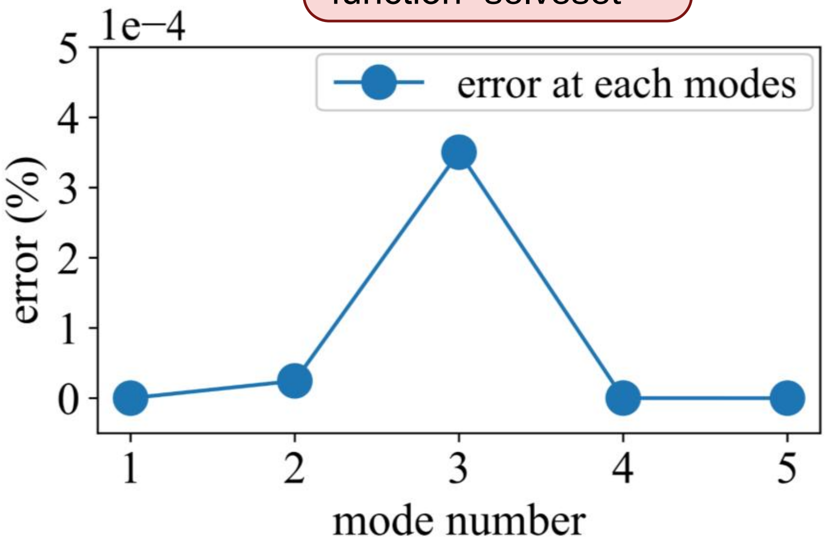

- **Step 5: Solve for new frequencies**

The new natural frequencies f_2 in Hz are then calculated for the five modes in the model utilized.

$$f_2 = \begin{pmatrix} 86 & 583 & 917 & 1602 & 1330221 \end{pmatrix}$$

Generalized Eigenvalue and LEMP

- Beam frequencies at each nodes on addition of roller at node 4 for first five modes

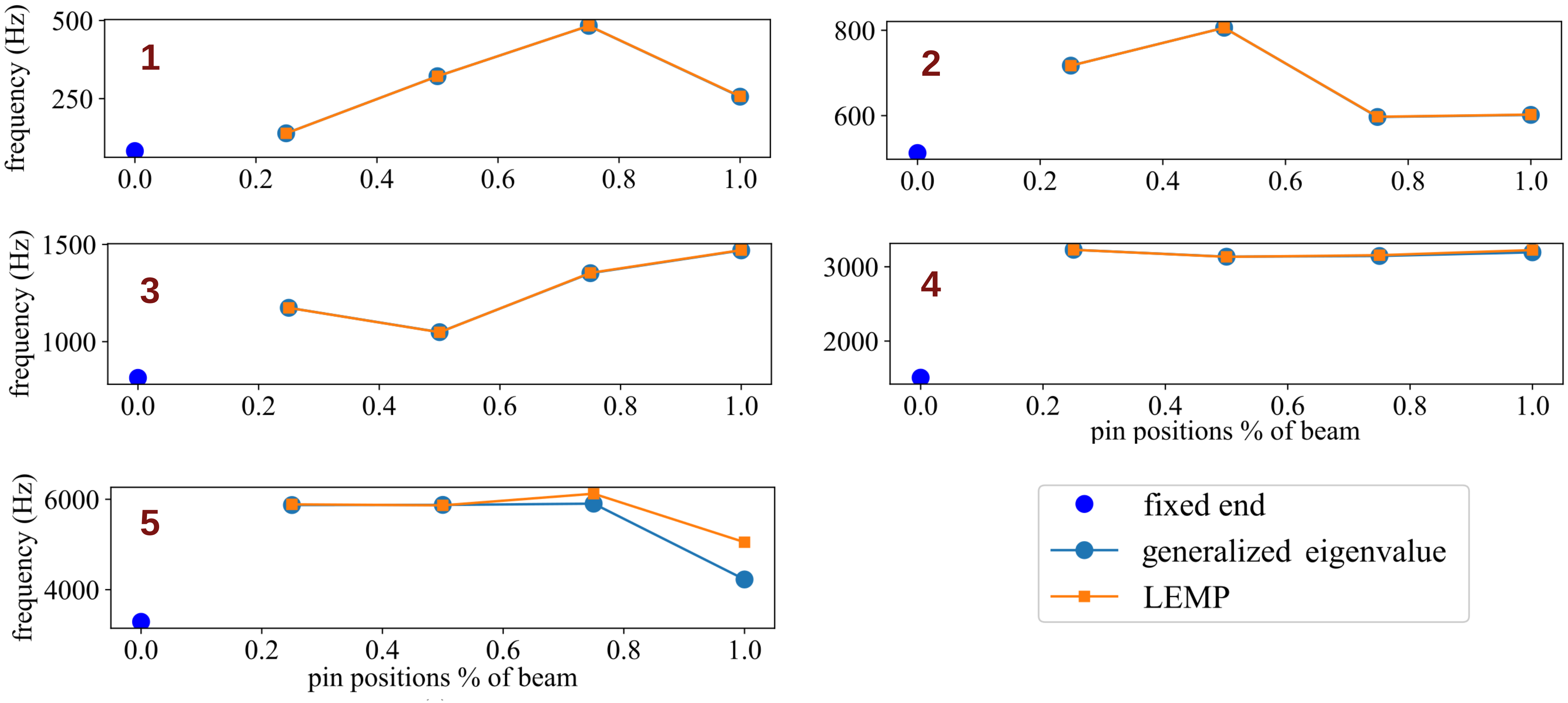

Generalized Eigenvalue and LEMP

- SNR & Error

mode	mean absolute error (Hz)	SNR $_{dB}$
1	0.2989	30.02
2	0.3193	33.38
3	0.5575	33.54
4	9.8136	25.10
5	262.80	13.18

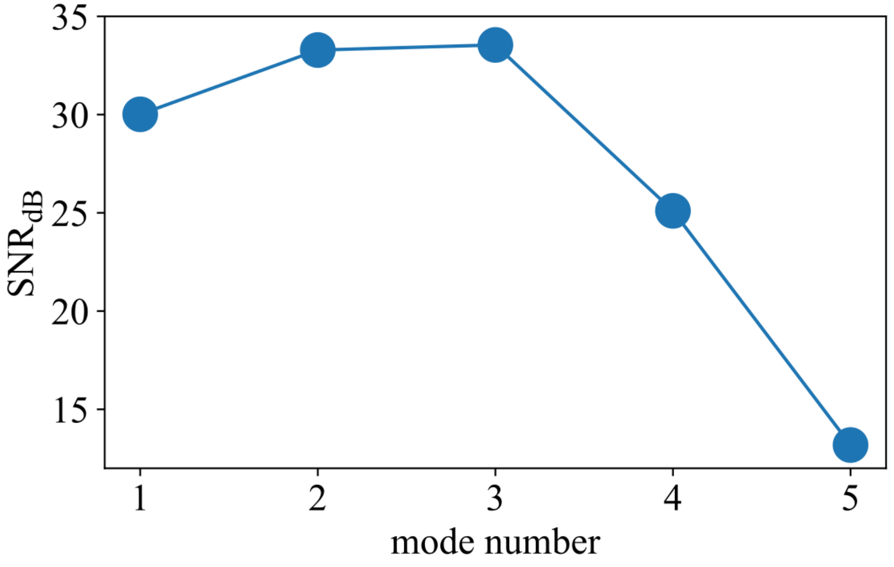

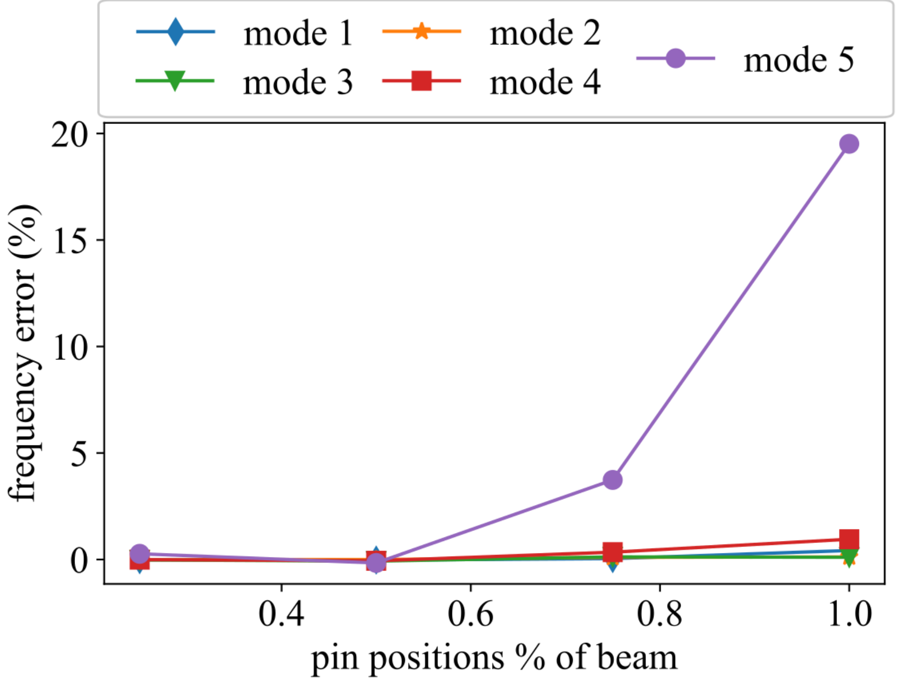

LEMP Algorithm Timing study

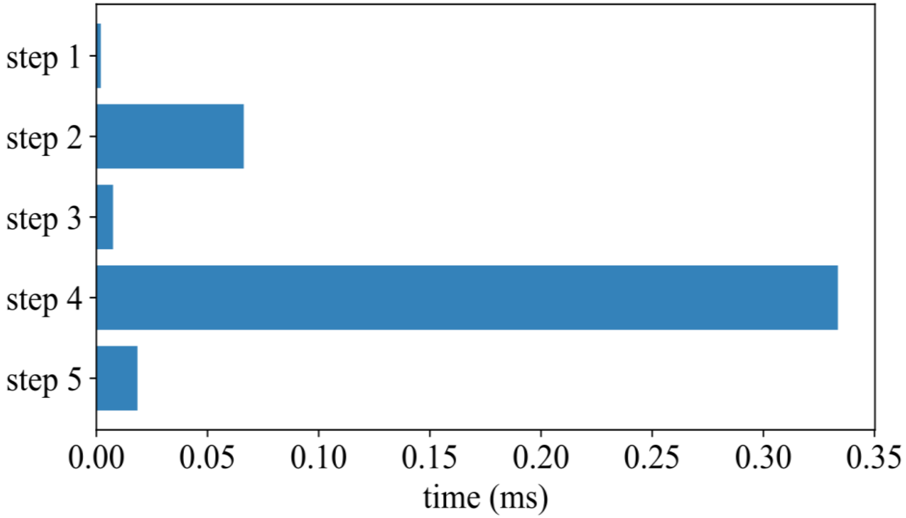

Timing for each step

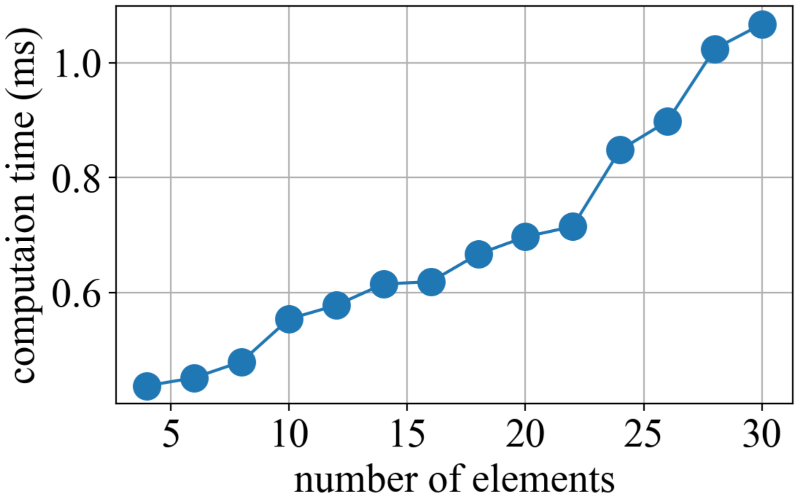

Timing with element number 4 to 30.

- Increasing the nodes increase the accuracy of the model
- <29 nodes achieves the 1ms times constraint

Contents

Model Updating Process

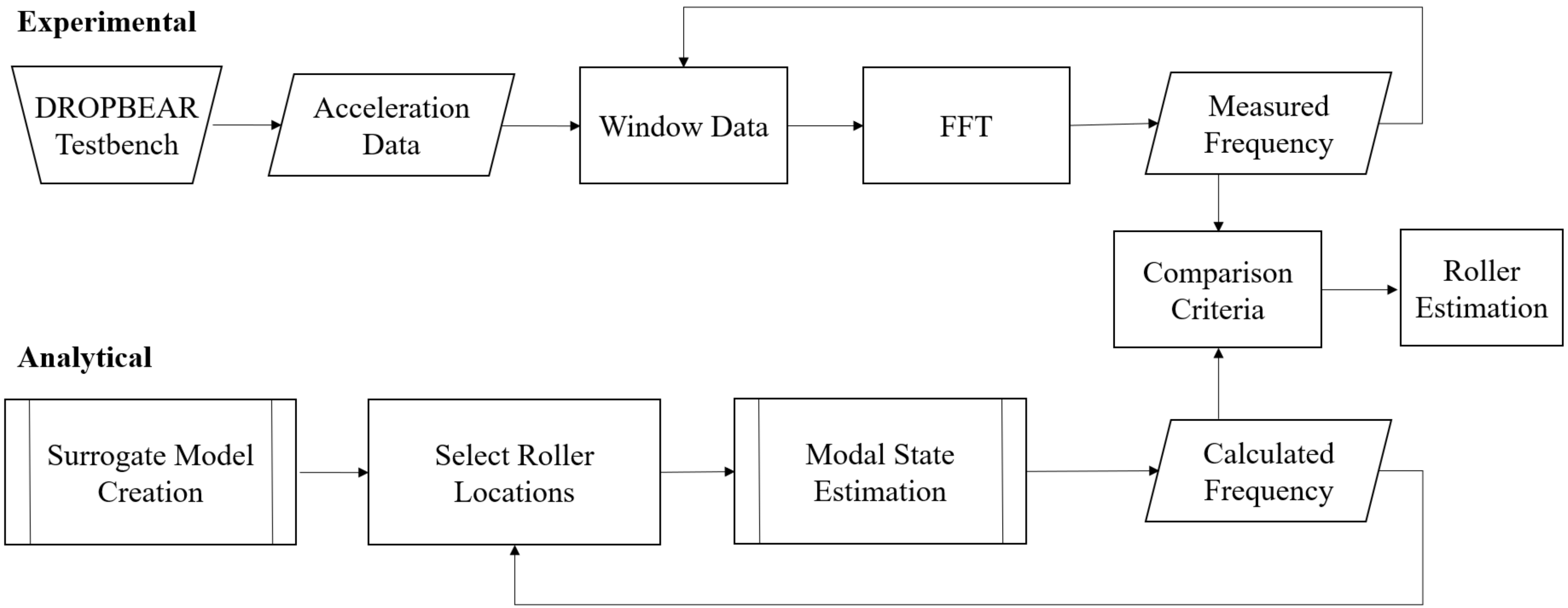

Experimental System used for Validation

- The Dynamic Reproduction of Projectiles in Ballistic Environments for Advanced Research (DROPBEAR) was used to generate the experimental data in this work.

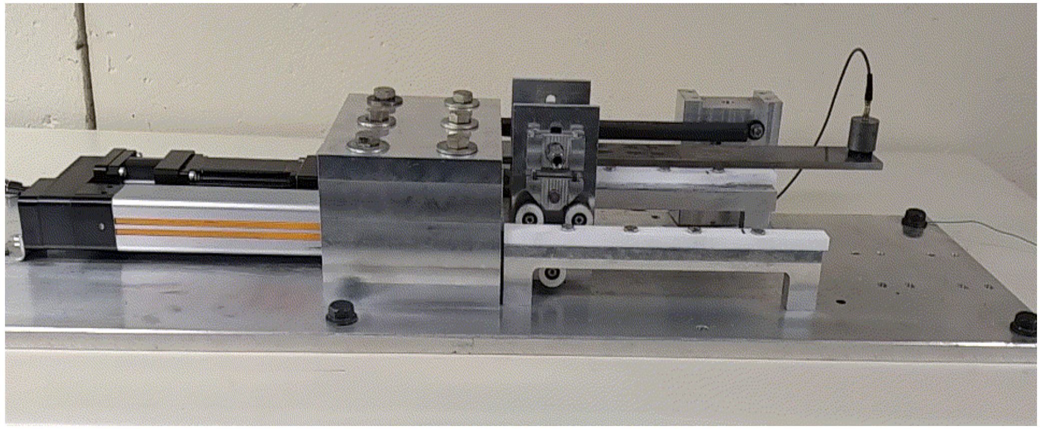

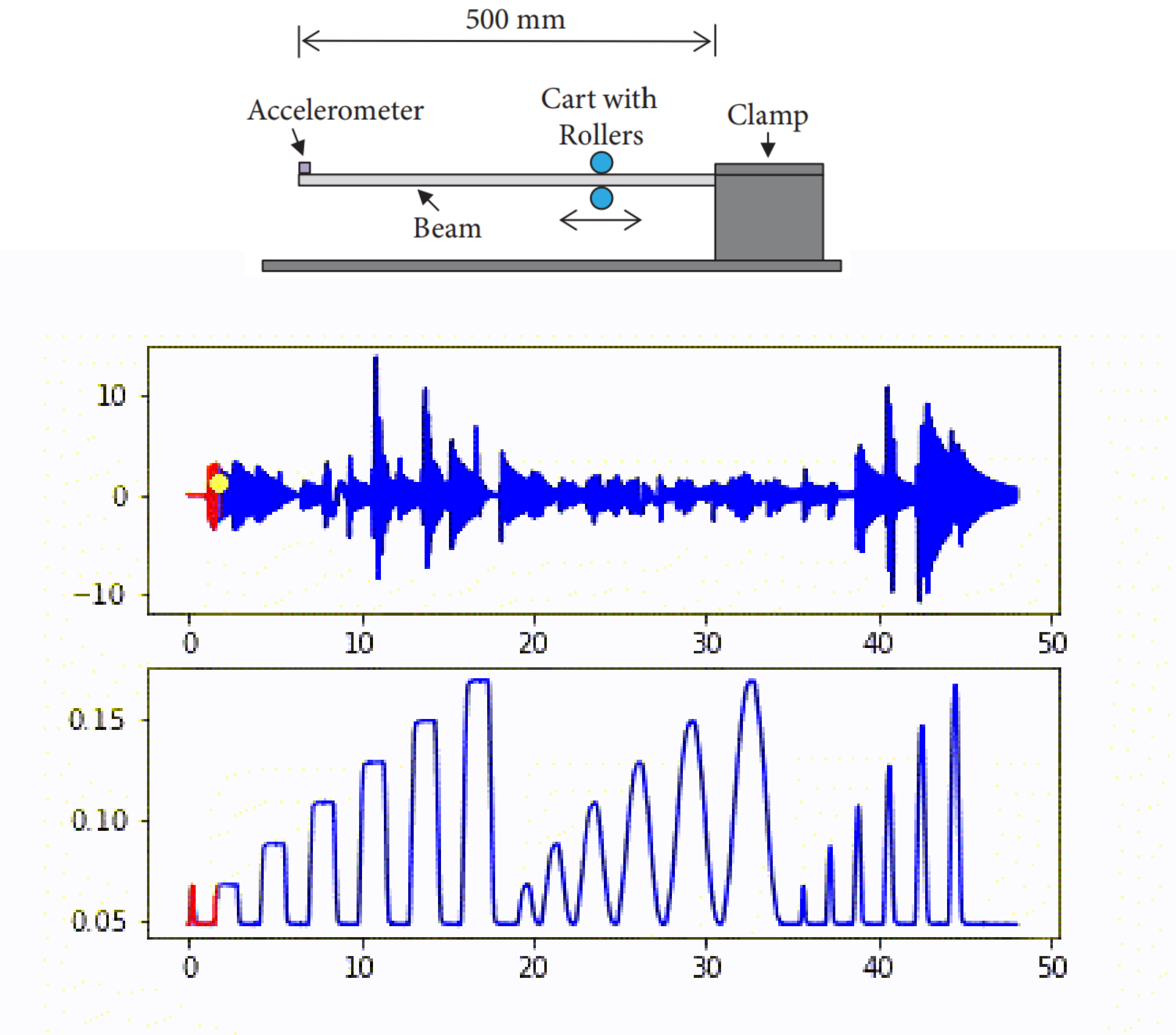

Joyce, B., Dodson, J., Laflamme, S., & Hong, J. *An experimental test bed for developing high-rate structural health monitoring methods*. Shock and Vibration, 2018.

Analytical: Probabilistic Roller Location Selection (Sampling)

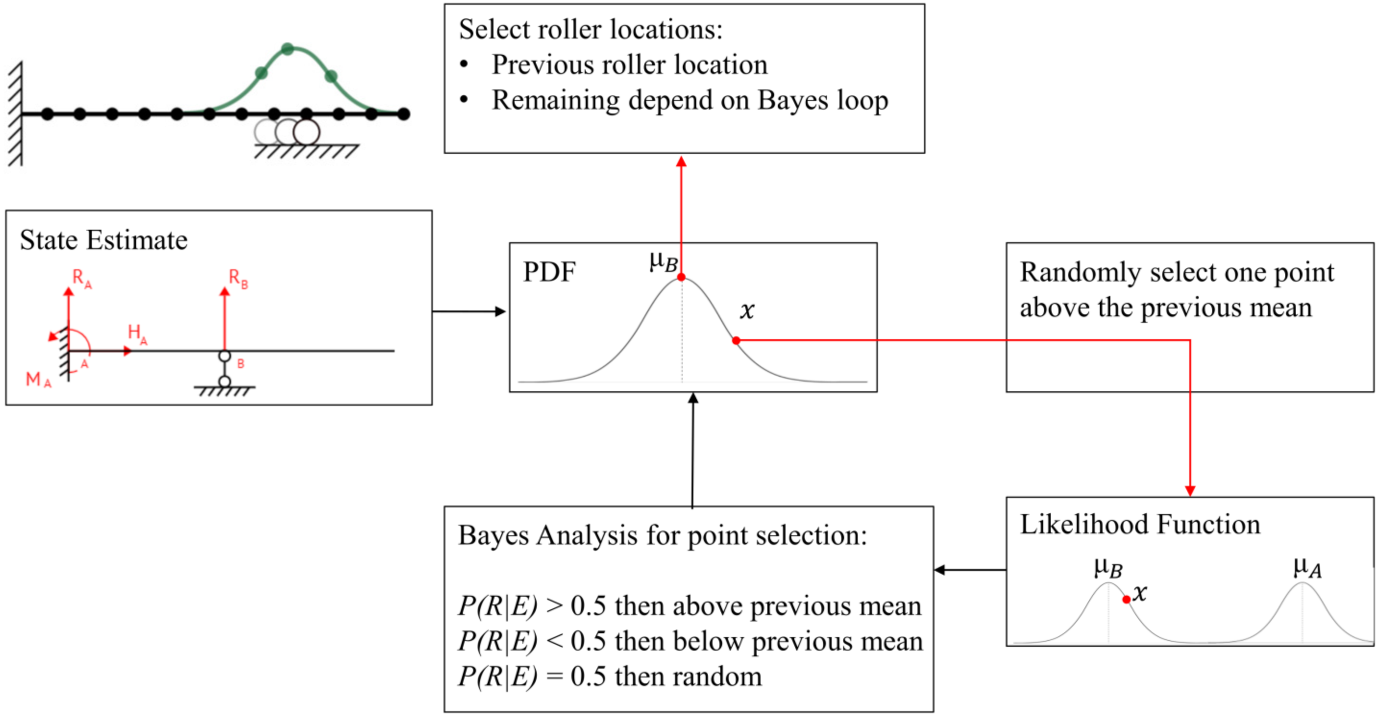

Comparison Criteria

Error Minimization

Least square regression

selected roller locations

$$X = \begin{bmatrix} x_1 & 1 \\ x_2 & 1 \\ x_3 & 1 \end{bmatrix}$$

min

$$Y = \begin{bmatrix} \omega_1 - \omega_{\text{true}} \\ \omega_2 - \omega_{\text{true}} \\ \omega_3 - \omega_{\text{true}} \end{bmatrix}$$

$$\begin{bmatrix} a \\ b \end{bmatrix} = (X^T X)^{-1} X^T Y$$

$$x_c = \begin{cases} x_{\min} & -{}^{b}/_{a} < x_{\min} \\ x_{\max} & -{}^{b}/_{a} > x_{\max} \\ -{}^{b}/_{a} & \text{elsewhere} \end{cases}$$

Where a and b are regression parameters such that $\omega - \omega_{\text{true}} = ax + b$. Therefore, $\omega = \omega_{\text{true}}$ when $x = -{}^{b}/_{a}$.

DROPBEAR Roller Location Estimation

21-node beam model

Error Minimization

Least square regression

Generalized Eigenvalue

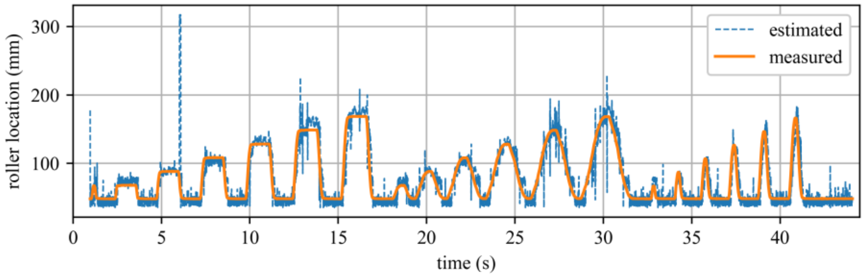

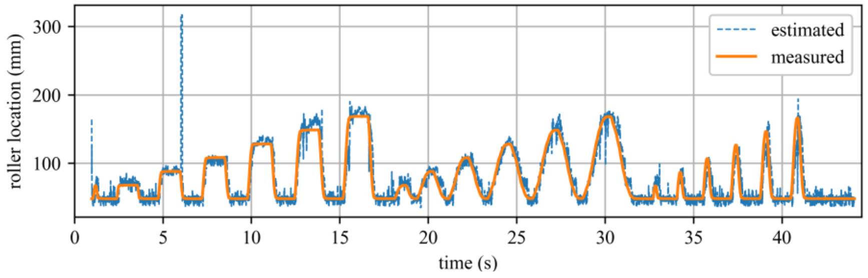

LEMP estimations

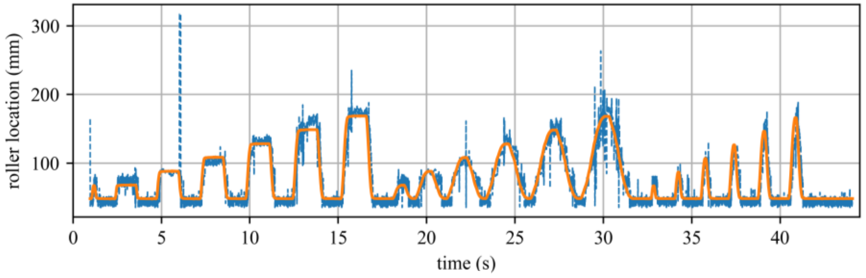

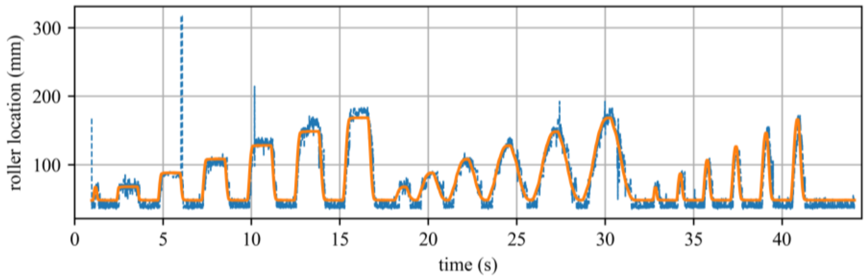

LEMP estimations alongside Bayesian search space.

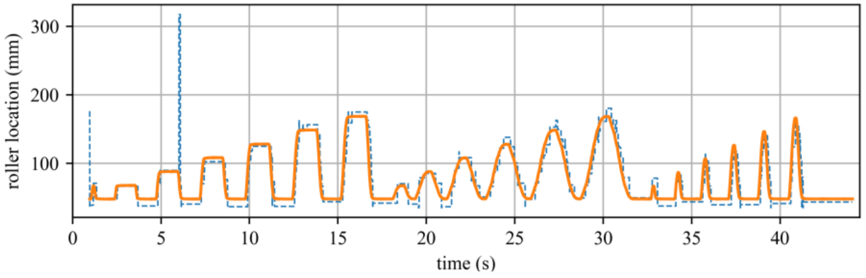

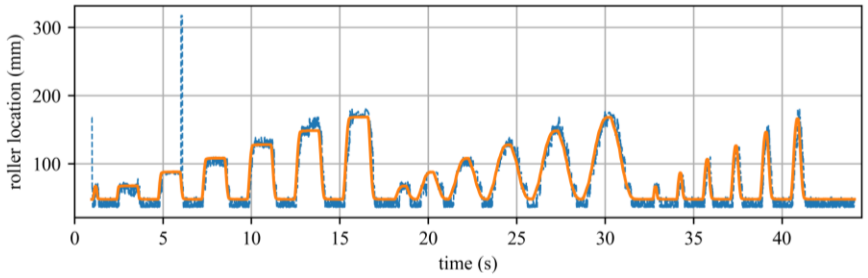

DROPBEAR Roller Location Estimation

LEMP estimate

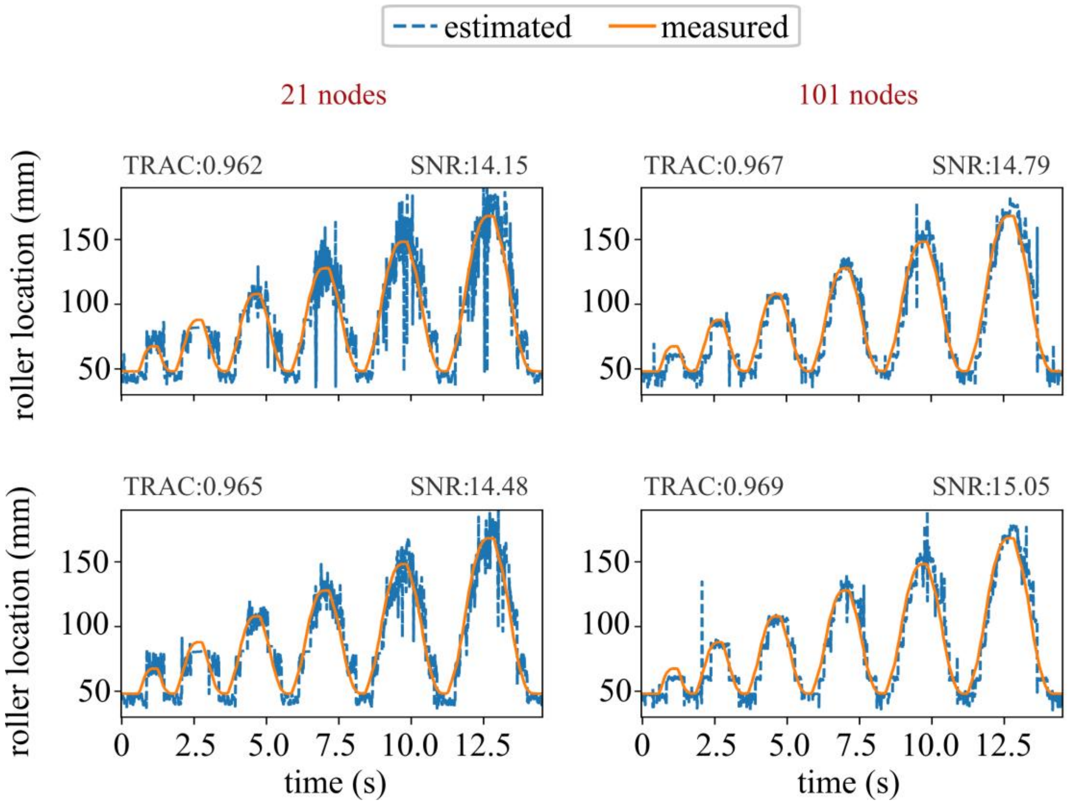

Error Minimization

Least square regression

21-node beam model extended view

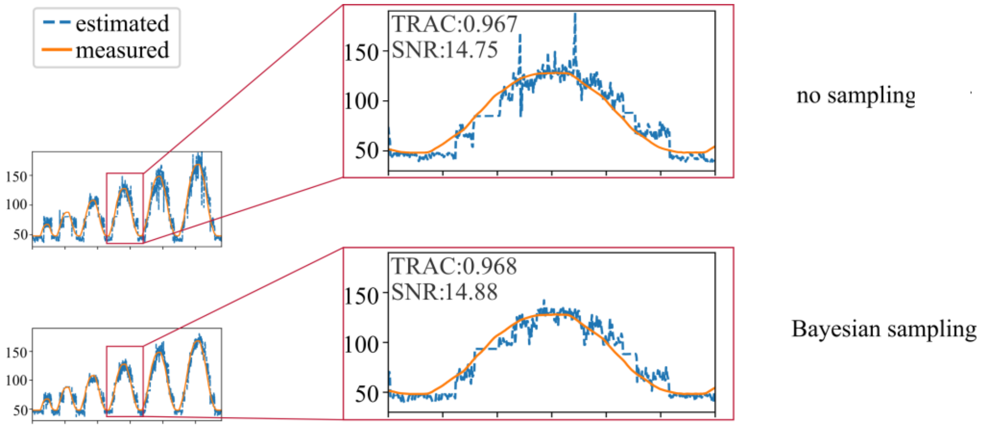

Timing Results

Error Minimization

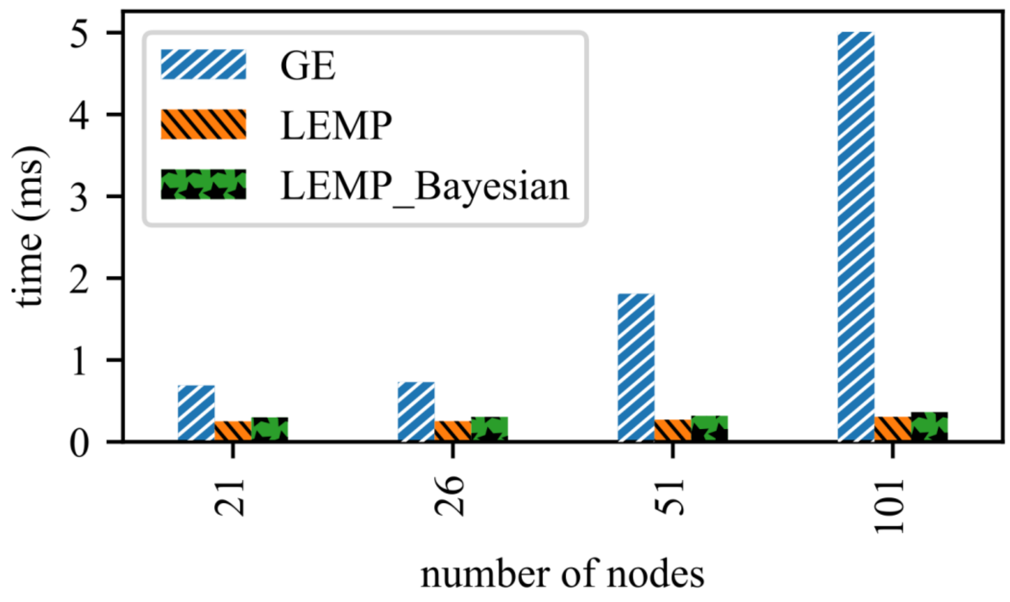

Least square regression

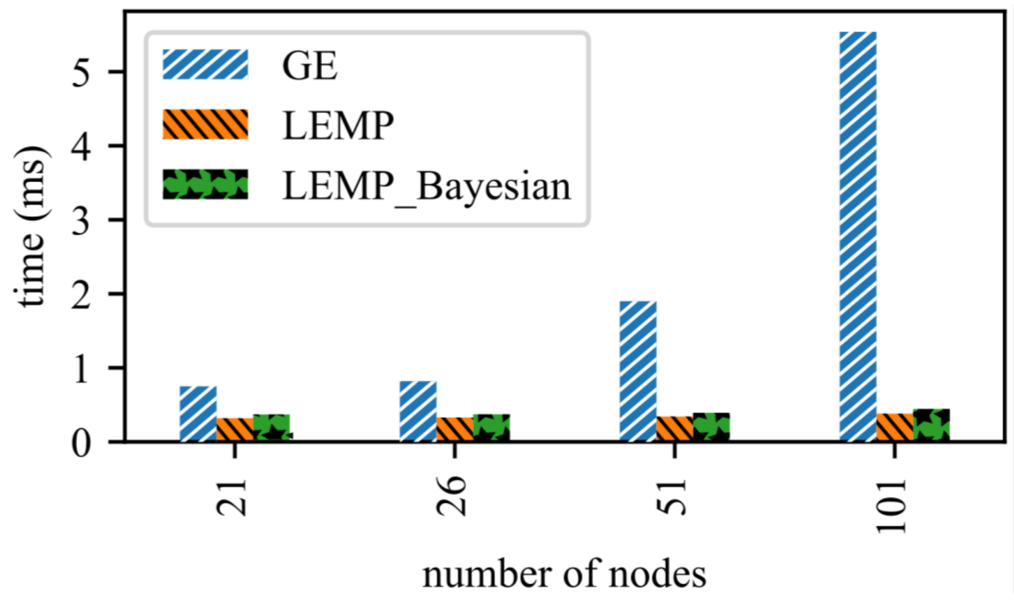

Timing Results

Solver time for the Generalize Eigenvalue and LEMP

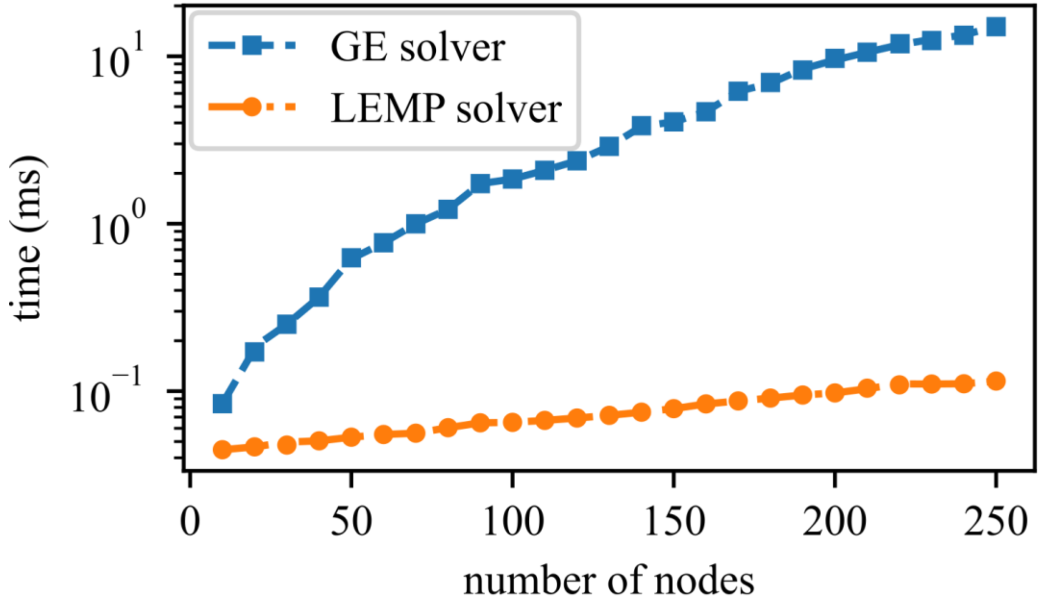

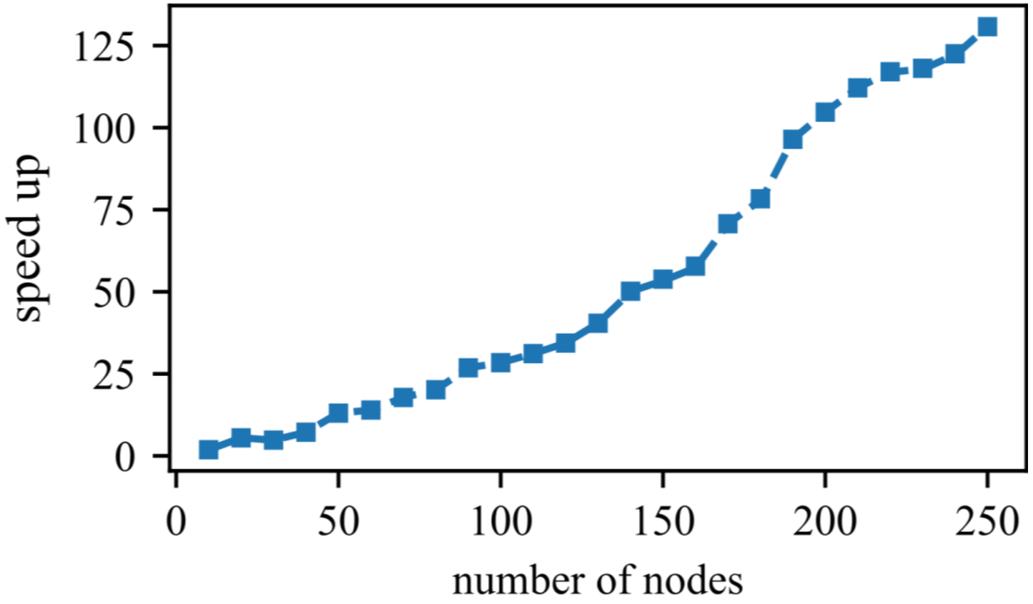

Optimal modal Configuration

MAE

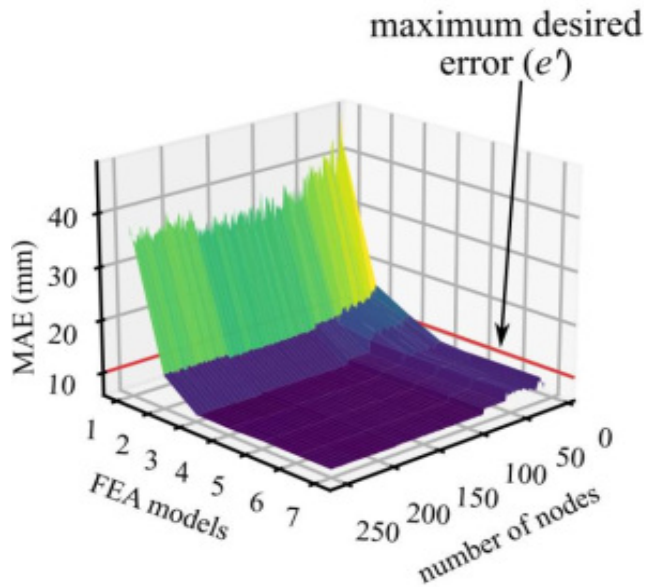

iteration time

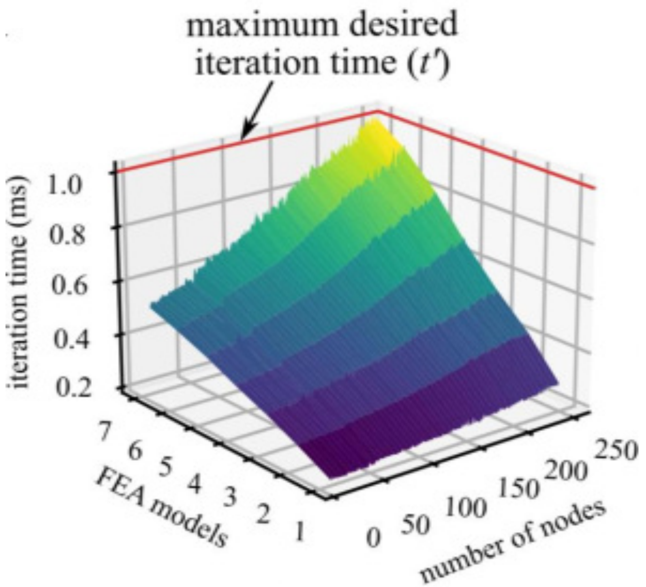

Optimal configuration

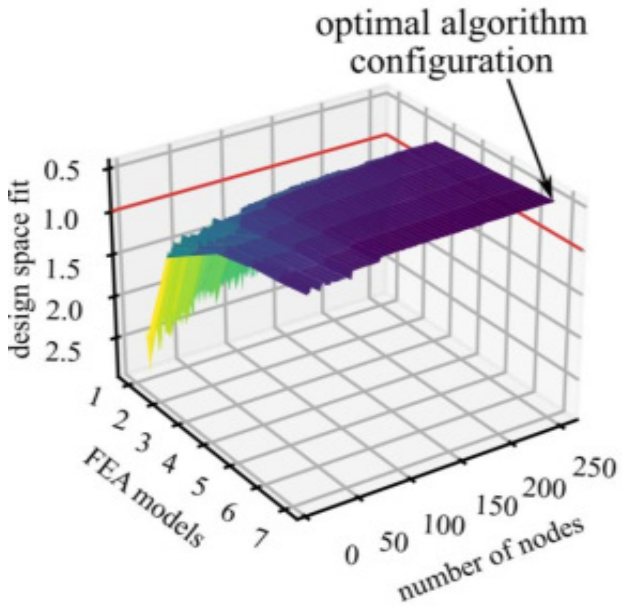

Contents

1D vs 2D Structural representation

1D

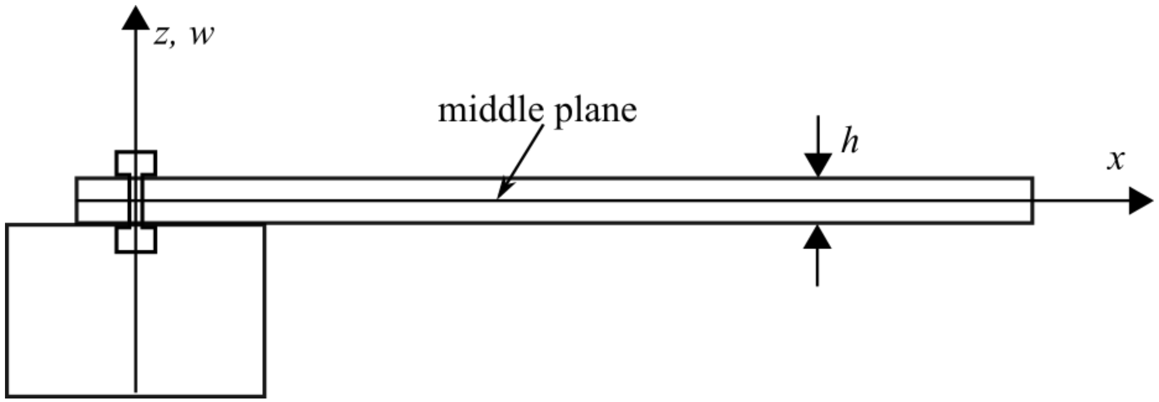

2D

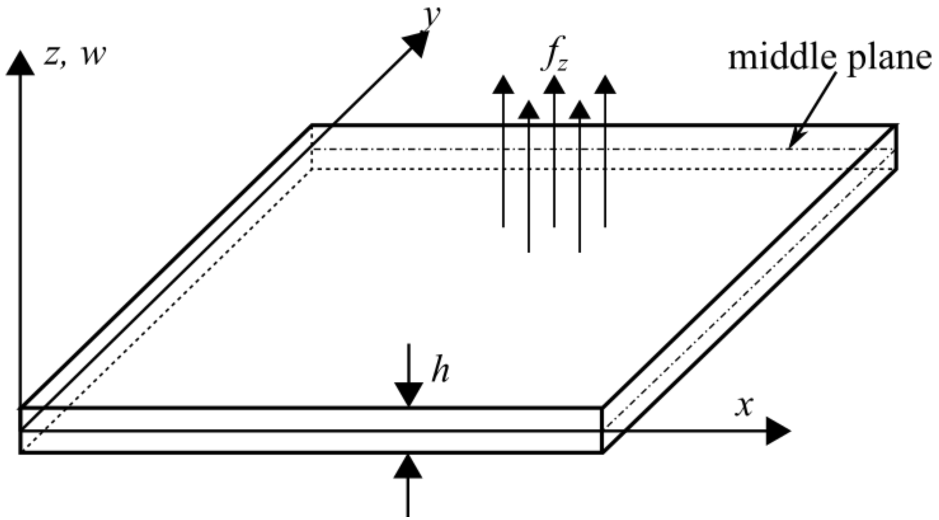

1D vs 2D Node construction

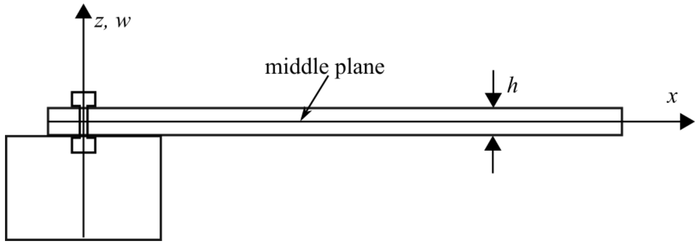

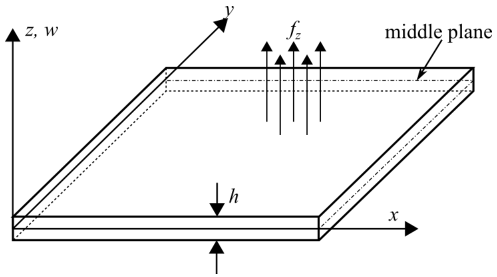

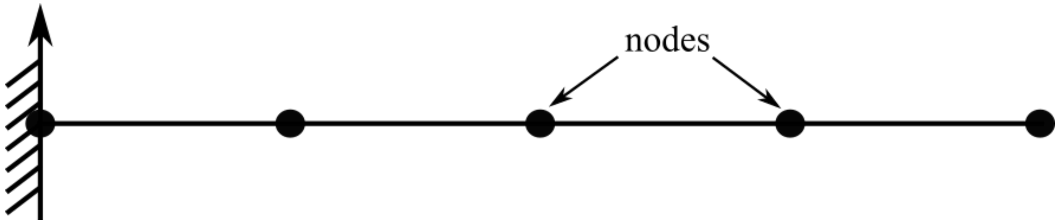

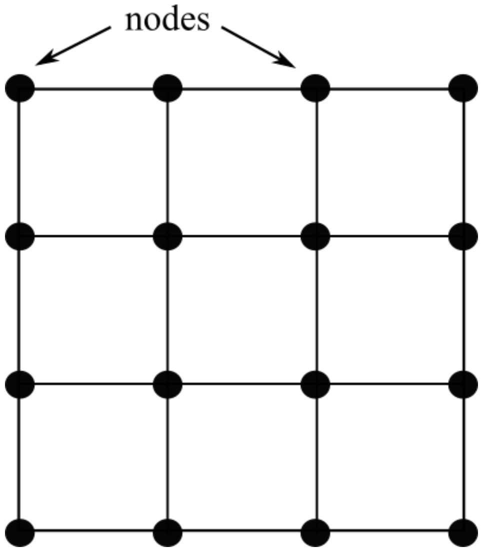

2D Model Formulation

Shell element = solid element + plate element

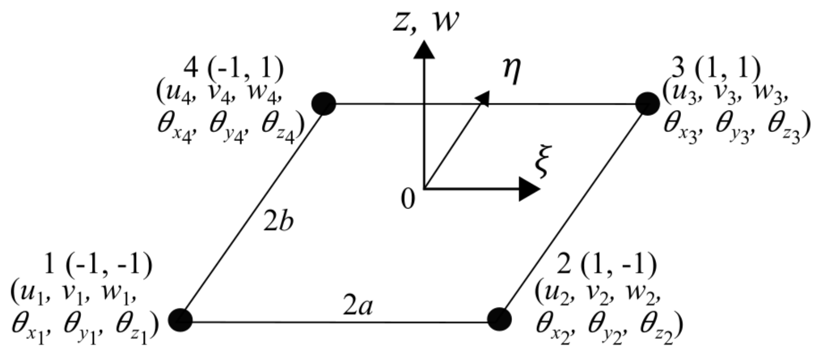

Three translational displacements in the *x*, *y*, and *z* directions, and three rotational deformations with respect to the *x*, *y*, and *z* axes.

$$\mathbf{d_e} = \begin{Bmatrix} \mathbf{d}_1 \\ \mathbf{d}_2 \\ \mathbf{d}_3 \\ \mathbf{d}_4 \end{Bmatrix} \begin{matrix} \text{node 1} \\ \text{node 2} \\ \text{node 3} \\ \text{node 4} \end{matrix}$$

where $\mathbf{d}_i$ (i=1, 2, 3, 4) are the displacement vector at node *i*:

$$\mathbf{d}_i = \begin{Bmatrix} u_i \\ v_i \\ w_i \\ \theta_{xi} \\ \theta_{yi} \\ \theta_{zi} \end{Bmatrix} \begin{matrix} \text{displacement in } x \text{ direction} \\ \text{displacement in } y \text{ direction} \\ \text{displacement in } z \text{ direction} \\ \text{rotation about } x\text{-axis} \\ \text{rotation about } y\text{-}axis \\ \text{rotation about } z\text{-axis} \end{matrix}$$

2D Model Formulation

Modeling steps

1. Construction of shape functions matrix **N**

2. Formulation of the strain matrix for **2D element** B, and **2D plate**, B_I and B_O.

3. Calculation of k_e and m_e using shape functions N and strain matrix in step 2.

2D Model Formulation

STEP 1. Construction of shape functions matrix N that satisfies Eqs. 1 and 2

2D element

$$\mathbf{N}_e = \begin{bmatrix} N_1 & 0 & N_2 & 0 & N_3 & 0 & N_4 & 0 \\ 0 & N_1 & 0 & N_2 & 0 & N_3 & 0 & N_4 \end{bmatrix} \tag{1}$$

2D plate

$$\mathbf{N}_p = \begin{bmatrix} N_1 & 0 & 0 & N_2 & 0 & 0 & N_3 & 0 & 0 & N_4 & 0 & 0 \\ 0 & N_1 & 0 & 0 & N_2 & 0 & 0 & N_3 & 0 & 0 & N_4 & 0 \\ 0 & 0 & N_1 & 0 & 0 & N_2 & 0 & 0 & N_3 & 0 & 0 & N_4 \end{bmatrix} \tag{2}$$

<u>Subscript</u>

e – 2D element
p – 2D plate

2D Model Formulation

STEP 2. Formulation of the strain matrix for 2D element B, Eq. 3 and 2D plate, B_I and B_O shown in Eqs. 4 and 5.

2D element

$$\mathbf{B} = \mathbf{LN} = \frac{1}{4}\begin{bmatrix} -\frac{1-\eta}{a} & 0 & \frac{1-\eta}{a} & 0 & \frac{1+\eta}{a} & 0 & -\frac{1+\eta}{a} & 0 \\ 0 & -\frac{1-\xi}{b} & 0 & -\frac{1+\xi}{b} & 0 & \frac{1+\xi}{b} & 0 & \frac{1-\xi}{b} \\ -\frac{1-\xi}{b} & -\frac{1-\eta}{a} & -\frac{1+\xi}{b} & \frac{1-\eta}{a} & \frac{1+\xi}{b} & \frac{1+\eta}{a} & \frac{1-\xi}{b} & -\frac{1+\eta}{a} \end{bmatrix} \qquad (3)$$

2D plate

$$\mathbf{B}^{\mathrm{I}} = \begin{bmatrix} \mathbf{B}_1^{\mathrm{I}} & \mathbf{B}_2^{\mathrm{I}} & \mathbf{B}_3^{\mathrm{I}} & \mathbf{B}_4^{\mathrm{I}} \end{bmatrix}, \qquad \mathbf{B}_{\mathrm{j}}^{\mathrm{I}} = \begin{bmatrix} 0 & 0 & -\partial N_j/\partial x \\ 0 & \partial N_j/\partial x & 0 \\ 0 & \partial N_j/\partial y & -\partial N_j \partial y \end{bmatrix} \qquad (4)$$

$$\mathbf{B}^{\mathrm{O}} = \begin{bmatrix} \mathbf{B}_1^{\mathrm{O}} & \mathbf{B}_2^{\mathrm{O}} & \mathbf{B}_3^{0} & \mathbf{B}_4^{0} \end{bmatrix}, \qquad \mathbf{B}_{\mathrm{j}}^{\mathrm{O}} = \begin{bmatrix} \partial N_j/\partial x & 0 & N_j \\ \partial N_j/\partial y & -N_j & 0 \end{bmatrix} \qquad (5)$$

2D Model Formulation

STEP 3. Calculation of k_e and m_e using shape functions N and strain matrix in step 2. to obtain Eqs. 6 and 7.

mass matrix

$$\mathbf{m}_{\mathrm{e}} = \int_A h\rho \mathbf{N}^{\mathrm{T}}\mathbf{N}\mathrm{dA}, \qquad \mathbf{m}_{\mathrm{p}} = \int_{A_p} \mathbf{N}^{\mathrm{T}}\mathbf{I}\mathbf{N}\mathrm{dA} \quad (6)$$

$$\mathbf{I} = \begin{bmatrix} \rho h & 0 & 0 \\ 0 & \rho h^3/12 & 0 \\ 0 & 0 & \rho h^3/12 \end{bmatrix}$$

stiffness matrix

$$\mathbf{k}_{\mathrm{e}} = \int_A h\mathbf{B}^{\mathrm{T}}\mathbf{c}\mathbf{B}\mathrm{dA}, \qquad \mathbf{k}_{\mathrm{p}} = \int_{A_p} \frac{h^3}{12}\left[\mathbf{B}^{\mathrm{I}}\right]^{\mathrm{T}}\mathbf{c}\mathbf{B}^{\mathrm{I}}dA + \int_{A_p} \kappa h \left[\mathbf{B}^{\mathrm{O}}\right]^{\mathrm{T}}\mathbf{c}_s\mathbf{B}^{\mathrm{O}}dA \quad (7)$$

2D Model Formulation

Elements in the global coordinate system

$$\mathbf{K}_e = \mathbf{T}^T \mathbf{k}_e \mathrm{T}$$

$$\mathbf{M}_e = \mathbf{T}^T \mathbf{m}_e \mathbf{T}$$

$$\mathbf{T} = \begin{bmatrix} \mathbf{T}_3 & \mathbf{0} & \mathbf{0} & \mathbf{0} & \mathbf{0} & \mathbf{0} & \mathbf{0} & \mathbf{0} \\ \mathbf{0} & \mathbf{T}_3 & \mathbf{0} & \mathbf{0} & \mathbf{0} & \mathbf{0} & \mathbf{0} & \mathbf{0} \\ \mathbf{0} & \mathbf{0} & \mathbf{T}_3 & \mathbf{0} & \mathbf{0} & \mathbf{0} & \mathbf{0} & \mathbf{0} \\ \mathbf{0} & \mathbf{0} & \mathbf{0} & \mathbf{T}_3 & \mathbf{0} & \mathbf{0} & \mathbf{0} & \mathbf{0} \\ \mathbf{0} & \mathbf{0} & \mathbf{0} & \mathbf{0} & \mathbf{T}_3 & \mathbf{0} & \mathbf{0} & \mathbf{0} \\ \mathbf{0} & \mathbf{0} & \mathbf{0} & \mathbf{0} & \mathbf{0} & \mathbf{T}_3 & \mathbf{0} & \mathbf{0} \\ \mathbf{0} & \mathbf{0} & \mathbf{0} & \mathbf{0} & \mathbf{0} & \mathbf{0} & \mathbf{T}_3 & \mathbf{0} \\ \mathbf{0} & \mathbf{0} & \mathbf{0} & \mathbf{0} & \mathbf{0} & \mathbf{0} & \mathbf{0} & \mathbf{T}_3 \end{bmatrix}_{24\times 24}$$

$$\mathbf{T}_3 = \begin{bmatrix} l_x & m_x & n_x \\ l_y & m_y & n_y \\ l_z & m_z & n_z \end{bmatrix}_{3\times 3}$$

T is the transformation matrix

where *lk, mk* and *nk* (*k*=*x, y, z*) are direction cosines

Contents

2D Matrices Validation

Type	Poisson’s ration	Young’s modulus	density	length	width	thickness
Steel	0.3	200e9	7700 kg/m3	0.3 m	0.3 m	0.006 m

4 elements – 9 nodes

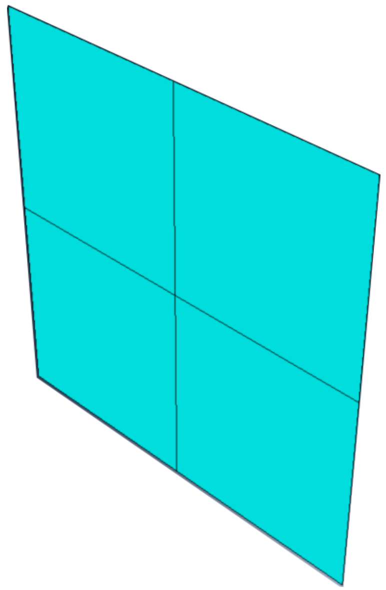

900 elements – 961 nodes

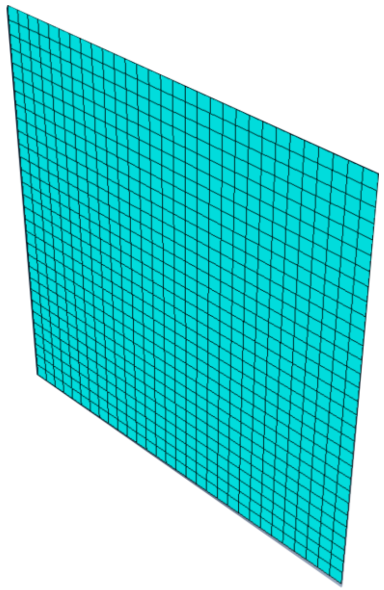

The plate was modeled in a free-free mode

FEA Simulations (4 elements plate)

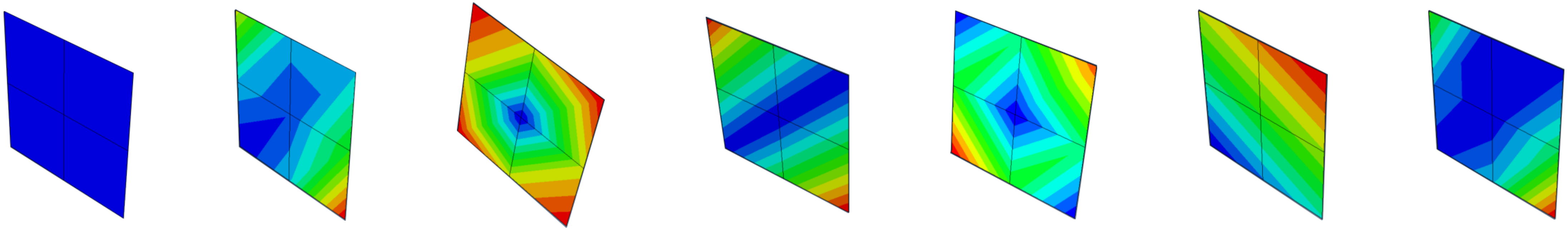

Mode 0: base state | Mode 1 | Mode 2 | Mode 3 | Mode 4 | Mode 5 | Mode 6

elastic mode

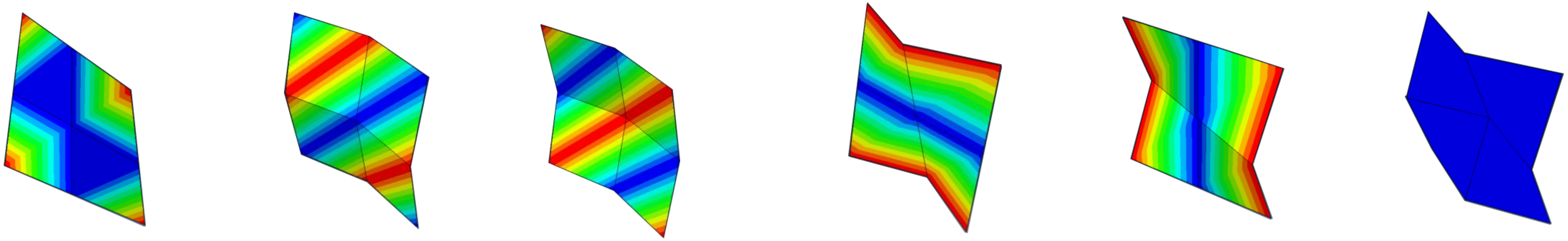

Mode 7 | Mode 8 | Mode 9 | Mode 10 | Mode 11 | Mode 12

FEA Simulations (900 elements plate)

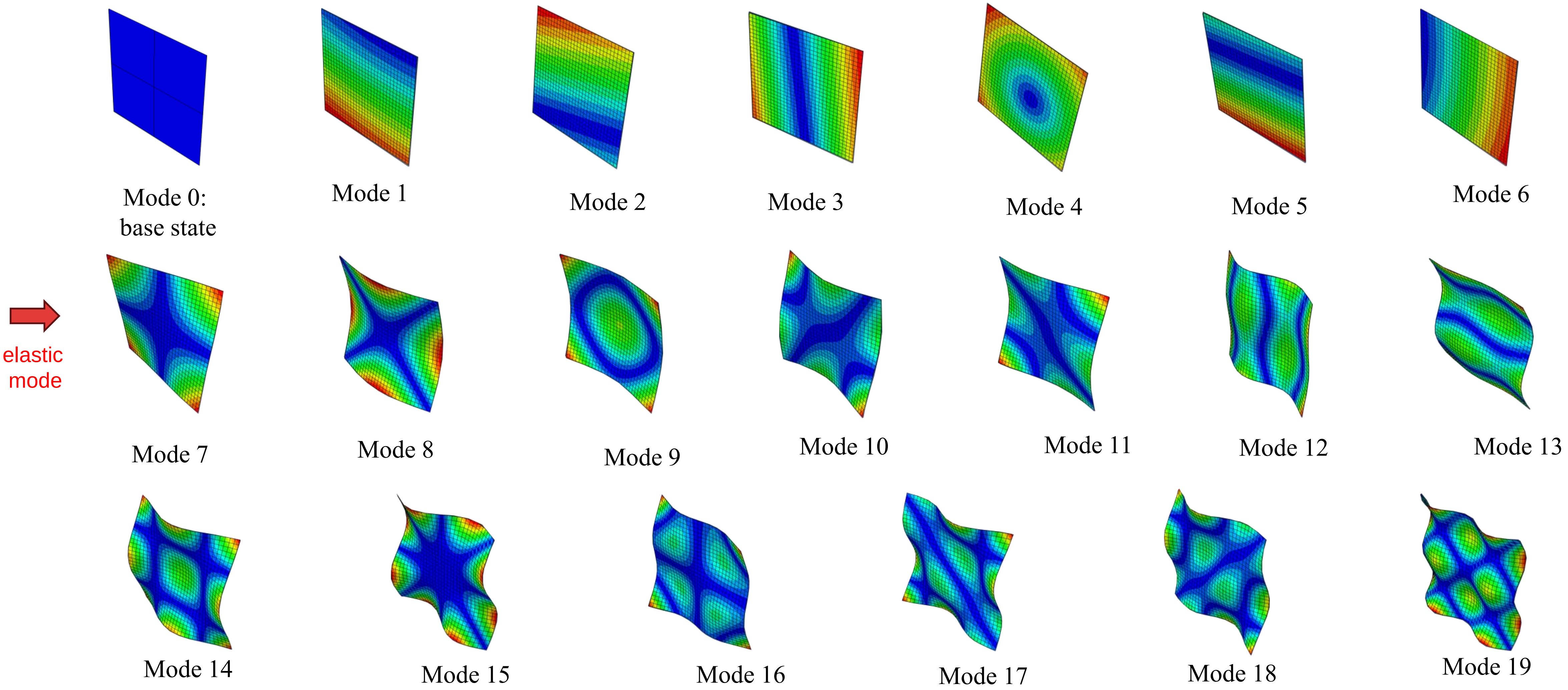

Modal frequencies

Step/Frame

Step Name	Description
Step-1	

4 elements

Frame

Index	Description
0	Increment 0: Base State
1	Mode 1: Value = -3.19909E-07 Freq = 0.0000 (cycles/time)
2	Mode 2: Value = -2.69152E-07 Freq = 0.0000 (cycles/time)
3	Mode 3: Value = -1.24332E-07 Freq = 0.0000 (cycles/time)
4	Mode 4: Value = -8.33534E-08 Freq = 0.0000 (cycles/time)
5	Mode 5: Value = -4.33065E-08 Freq = 0.0000 (cycles/time)
6	Mode 6: Value = -3.72529E-09 Freq = 0.0000 (cycles/time)
7	Mode 7: Value = 2.12713E+06 Freq = 232.12 (cycles/time)
8	Mode 8: Value = 5.66377E+06 Freq = 378.77 (cycles/time)
9	Mode 9: Value = 1.05068E+07 Freq = 515.89 (cycles/time)
10	Mode 10: Value = 1.41477E+07 Freq = 598.64 (cycles/time)
11	Mode 11: Value = 1.41477E+07 Freq = 598.64 (cycles/time)
12	Mode 12: Value = 3.52346E+07 Freq = 944.72 (cycles/time)

Step/Frame

Step Name	Description
Step-1	

900 elements

Frame

Index	Description
0	Increment 0: Base State
1	Mode 1: Value = 2.11708E-06 Freq = 2.31573E-04 (cycles/time)
2	Mode 2: Value = 3.40977E-06 Freq = 2.93888E-04 (cycles/time)
3	Mode 3: Value = 5.05996E-06 Freq = 3.58009E-04 (cycles/time)
4	Mode 4: Value = 6.18608E-06 Freq = 3.95847E-04 (cycles/time)
5	Mode 5: Value = 7.60294E-06 Freq = 4.38845E-04 (cycles/time)
6	Mode 6: Value = 1.44800E-05 Freq = 6.05625E-04 (cycles/time)
7	Mode 7: Value = 1.89263E+06 Freq = 218.95 (cycles/time)
8	Mode 8: Value = 4.05830E+06 Freq = 320.62 (cycles/time)
9	Mode 9: Value = 6.23002E+06 Freq = 397.25 (cycles/time)
10	Mode 10: Value = 1.26330E+07 Freq = 565.68 (cycles/time)
11	Mode 11: Value = 1.26330E+07 Freq = 565.68 (cycles/time)
12	Mode 12: Value = 3.95886E+07 Freq = 1001.4 (cycles/time)
13	Mode 13: Value = 3.95886E+07 Freq = 1001.4 (cycles/time)
14	Mode 14: Value = 4.20637E+07 Freq = 1032.2 (cycles/time)
15	Mode 15: Value = 5.01417E+07 Freq = 1127.0 (cycles/time)
16	Mode 16: Value = 6.26389E+07 Freq = 1259.6 (cycles/time)
17	Mode 17: Value = 1.15204E+08 Freq = 1708.3 (cycles/time)
18	Mode 18: Value = 1.15204E+08 Freq = 1708.3 (cycles/time)
19	Mode 19: Value = 1.46137E+08 Freq = 1924.0 (cycles/time)

2D Matrices Validation

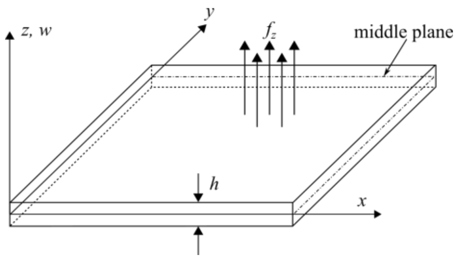

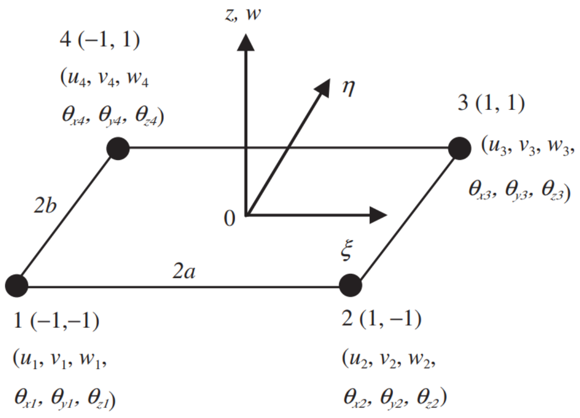

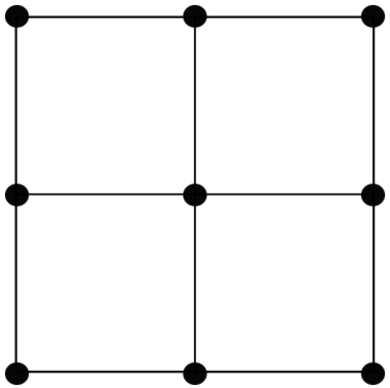

Mode	FEA	GE	Error (abs)
7	232.12	232.027	0.0093
8	378.77	379.044	0.274
9	515.89	515.983	0.0093
10	598.64	598.768	0.128
11	598.64	598.768	0.128
12	944.72	945.03	0.31

Single state change with GE and LEMP

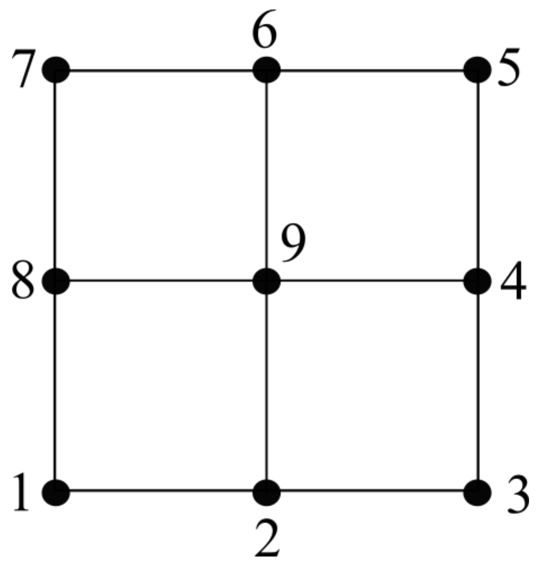

change in Stiffness value by 5e100 N/m at deflection (w) DOF of z-axis

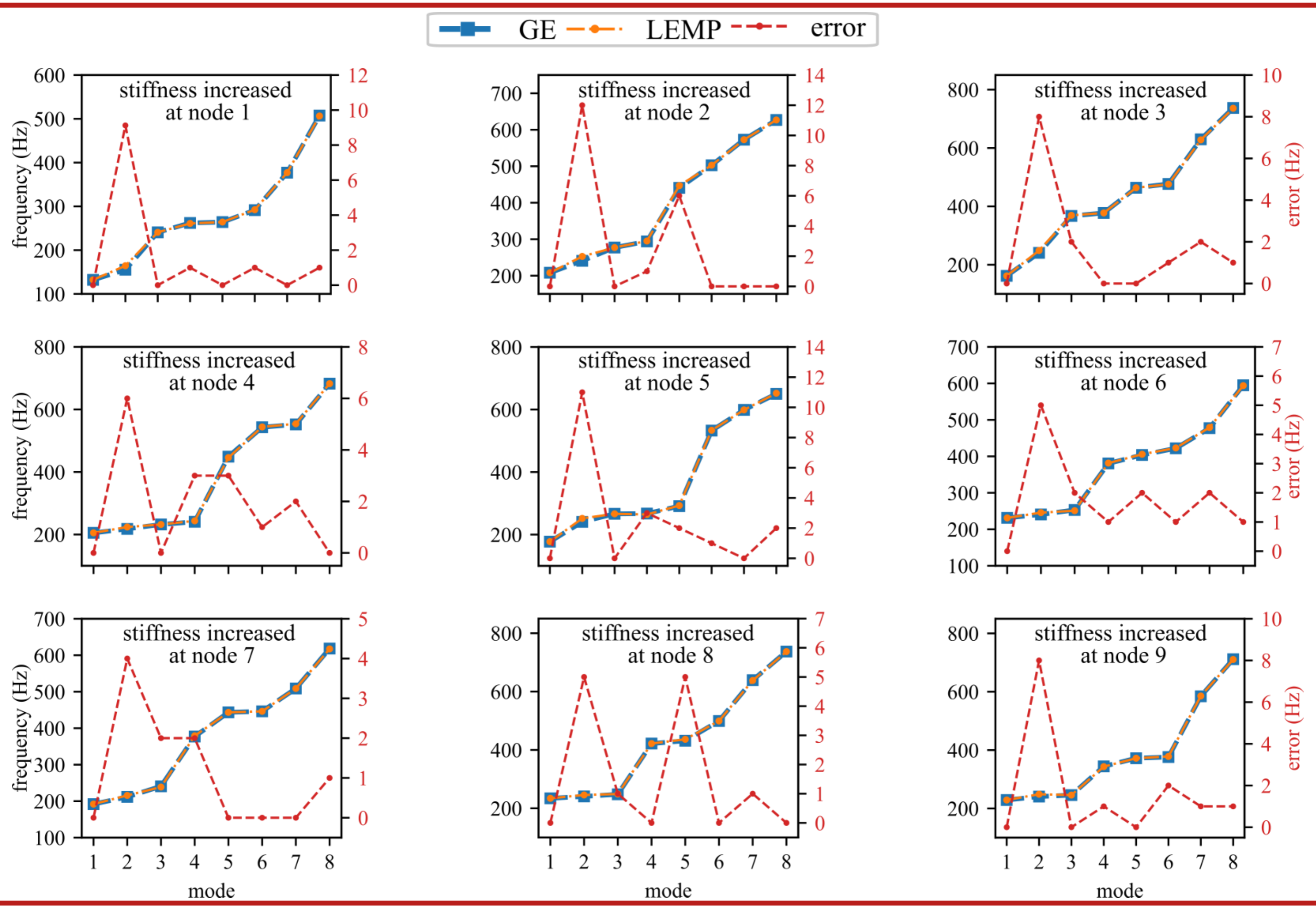

Single state change with GE and LEMP

Estimation Timing for GE and LEMP

single change calculated using:				generalized eigenvalue		LEMP		
no. of nodes	no. of element	DOF	matrix size	freq (Hz)	time GE (s)	freq (Hz)	time LEMP (s)	error (Hz)
9	4	54	54 x 54	232.027	0.001093	227.099	0.000384	4.928
16	9	96	96 x 96	228.458	0.00320	226.120	0.000456	2.338
25	16	150	150 x 150	224.914	0.009031	224.123	0.000458	0.791
36	25	216	216 x 216	222.886	0.024529	223.01	0.000464	-0.124
49	36	294	294 x 294	221.78	0.067579	222.1	0.000399	-0.32
64	49	384	384 x 384	221.599	0.212773	221.67	0.000475	-0.071
81	64	486	486 x 486	220.837	0.348656	220.610	0.000539	0.227
100	81	600	600 x 600	219.975	0.559744	219.41	0.000691	0.565
121	100	726	726 x 726	222.409	0.994675	221.919	0.000890	0.488
144	121	864	864 x 864	218.505	2.197694	217.68	0.001285	0.825
169	144	1014	1014 x 1014	219.147	4.075451	219.234	0.001523	-0.087

Up to 100 nodes, the LEMP algorithm can still achieve 691 μs while GE is already at 0.56 s.

Single state change with GE and LEMP

Model update accuracy and timing

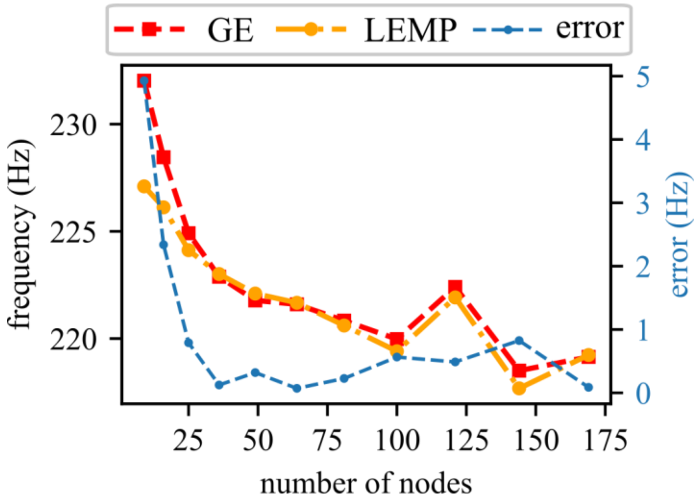

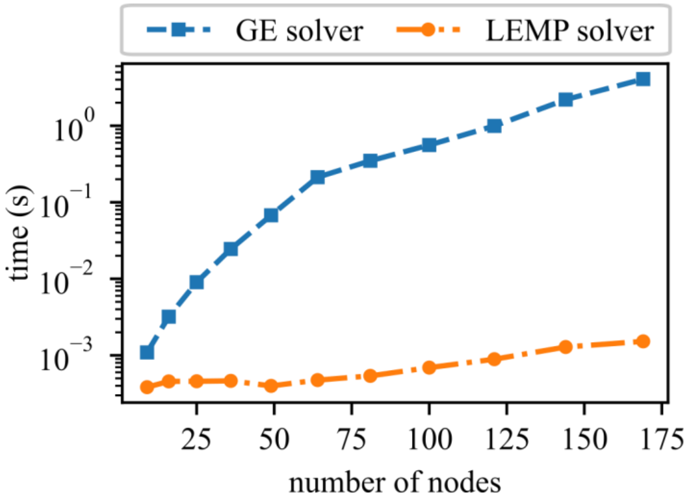

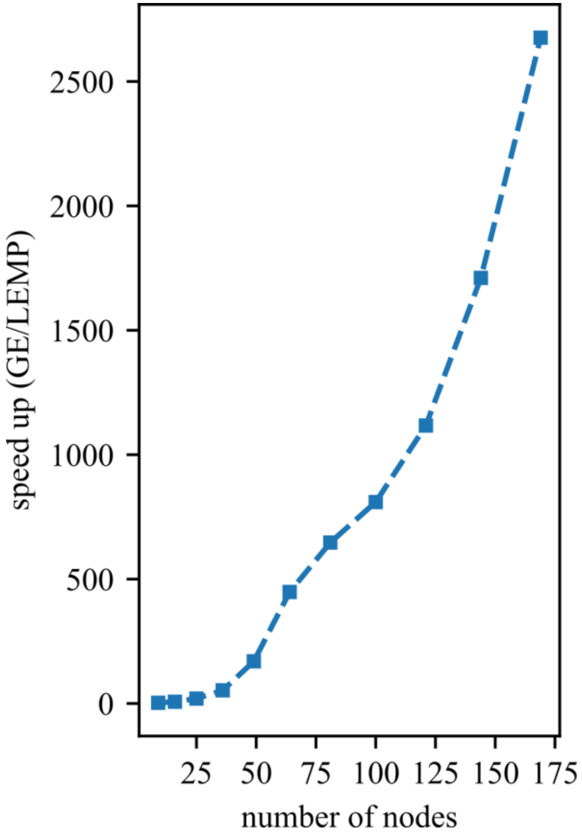

Only the first elastic mode was used for the frequency plot

Optimal Reduced model

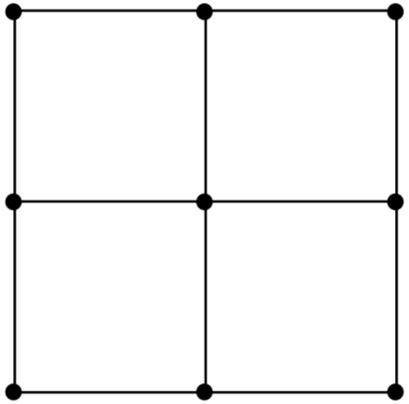

9 nodes

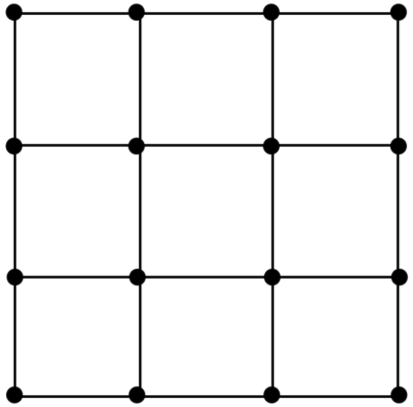

16 nodes

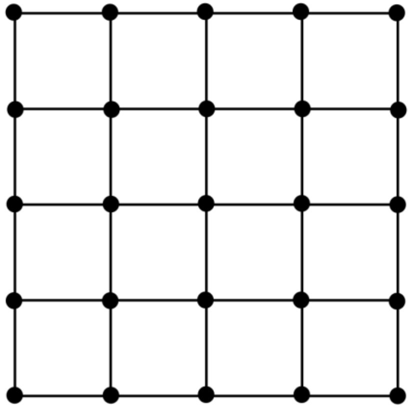

25 nodes

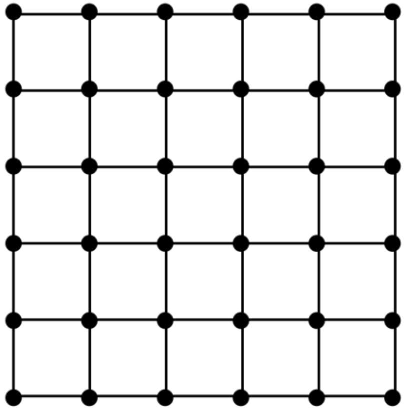

36 nodes

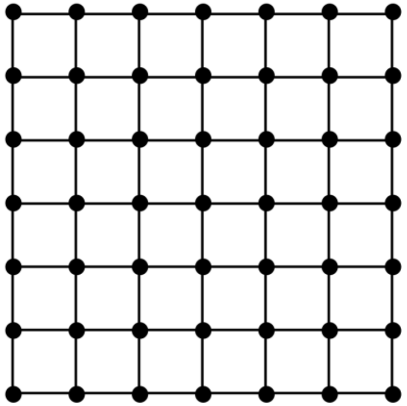

49 nodes

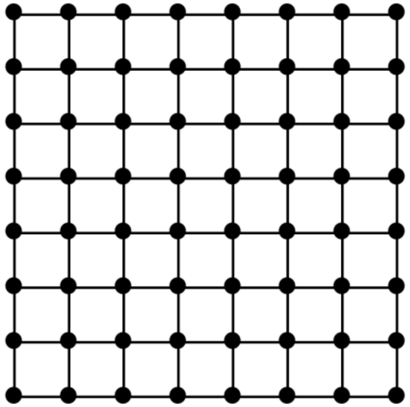

64 nodes

Free plate

Each reduced model are compared to a perfectly meshed free plate

Free plate

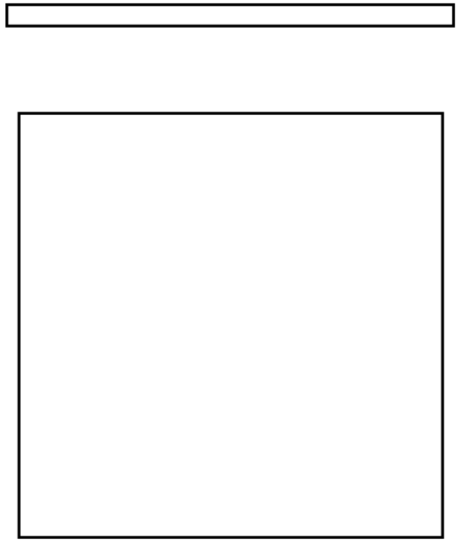

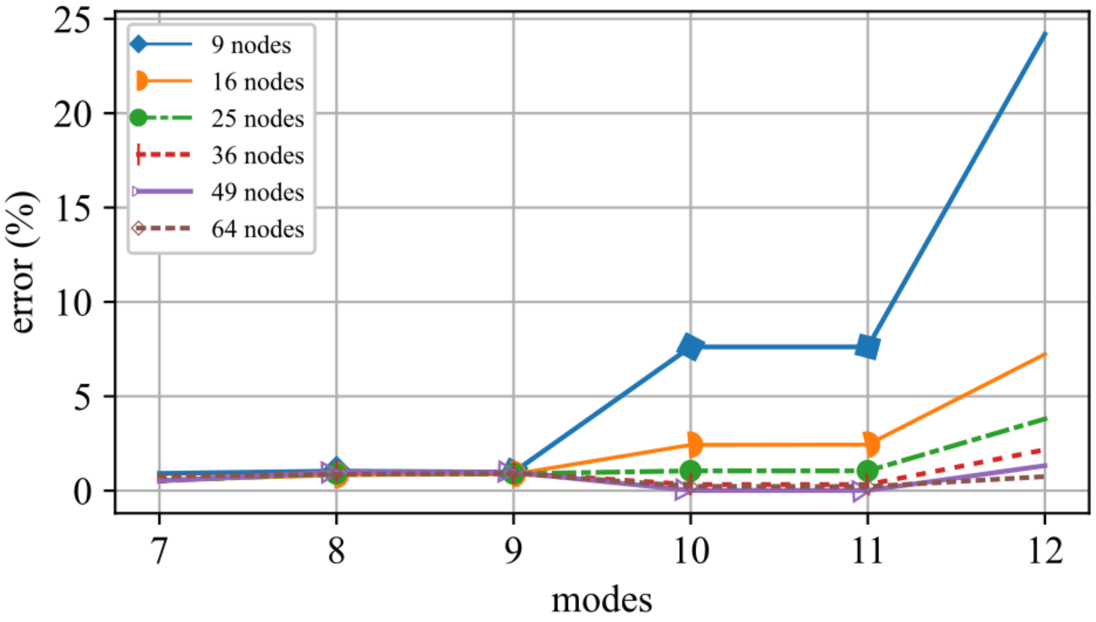

Cantilever plate

Each reduced model are compared to a perfectly meshed cantilever plate

Cantilever plate

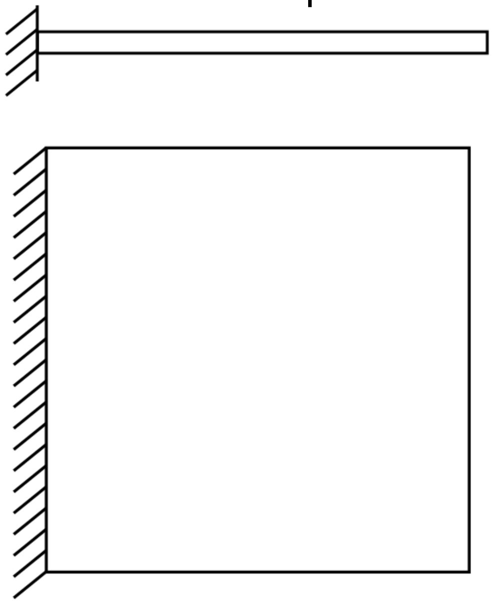

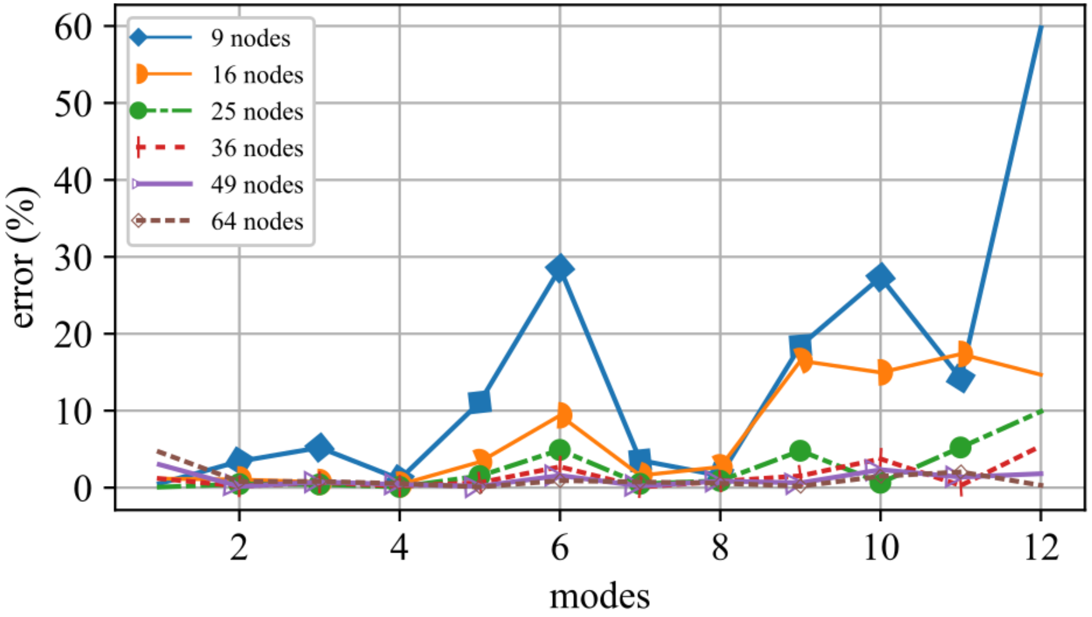

Free Plate to Cantilever Plate

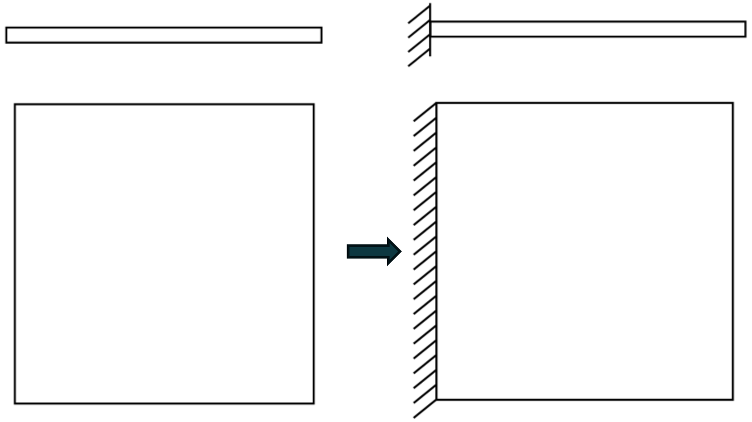

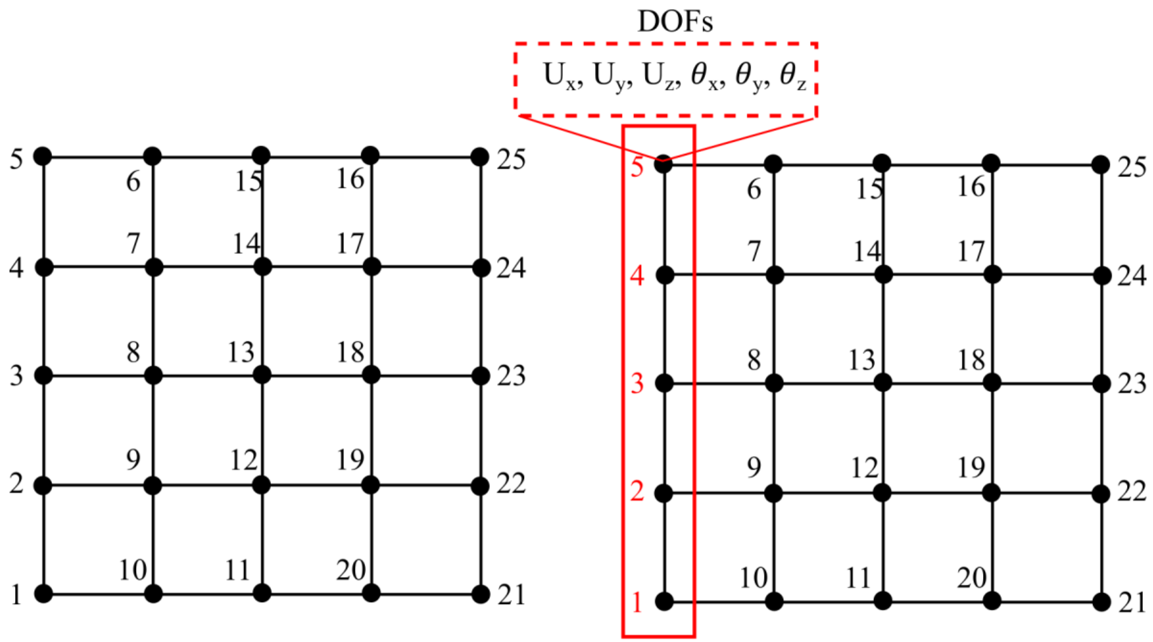

free plate nodal construction

fix nodes 1,2,3,4 and 5

Local change introduction

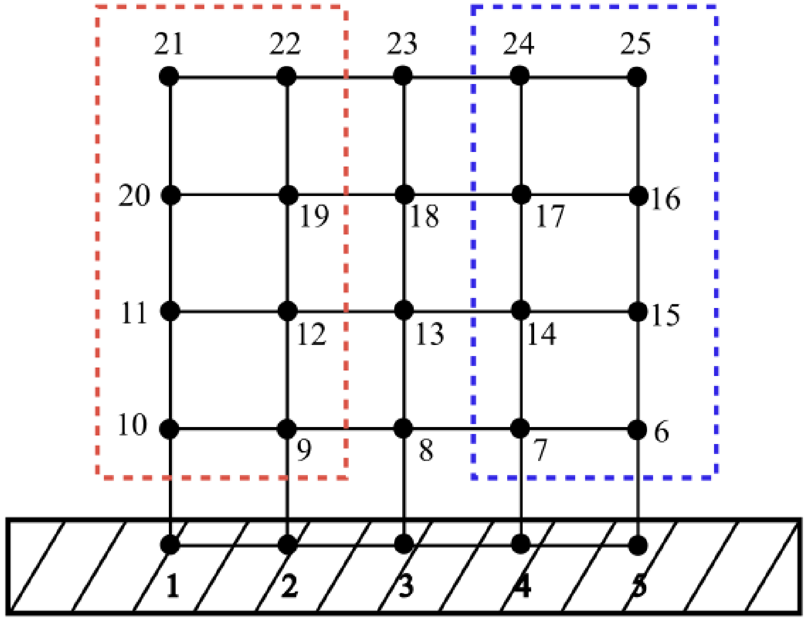

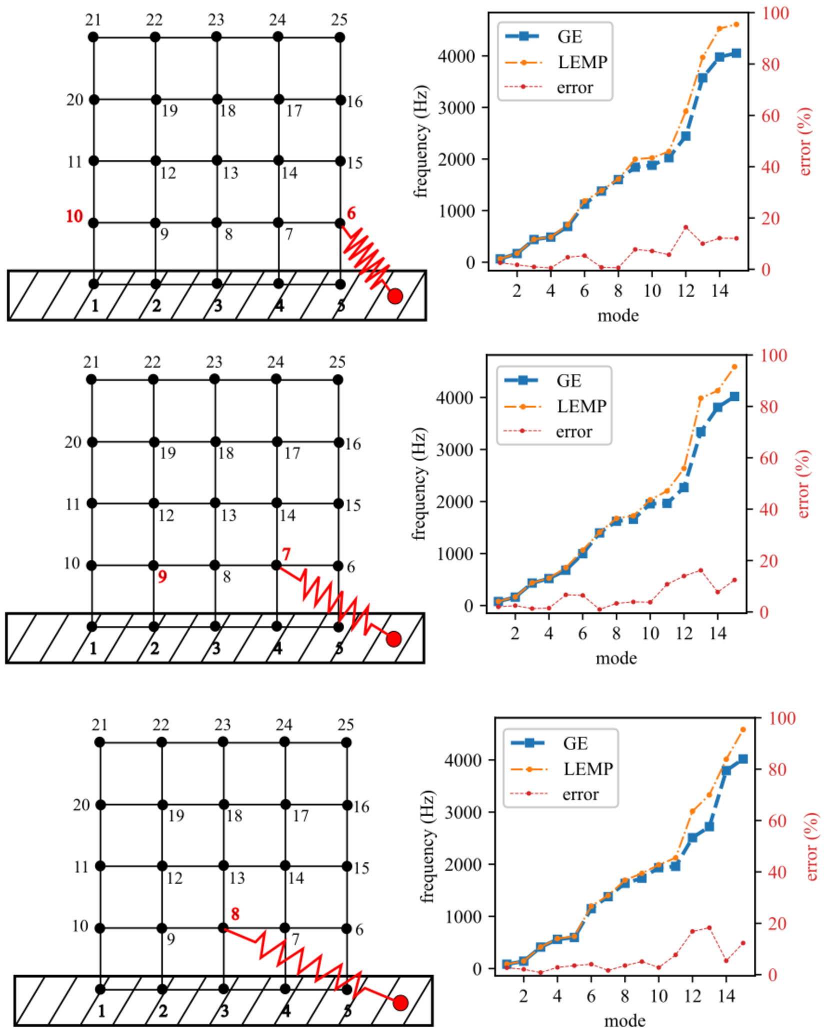

Local change introduction

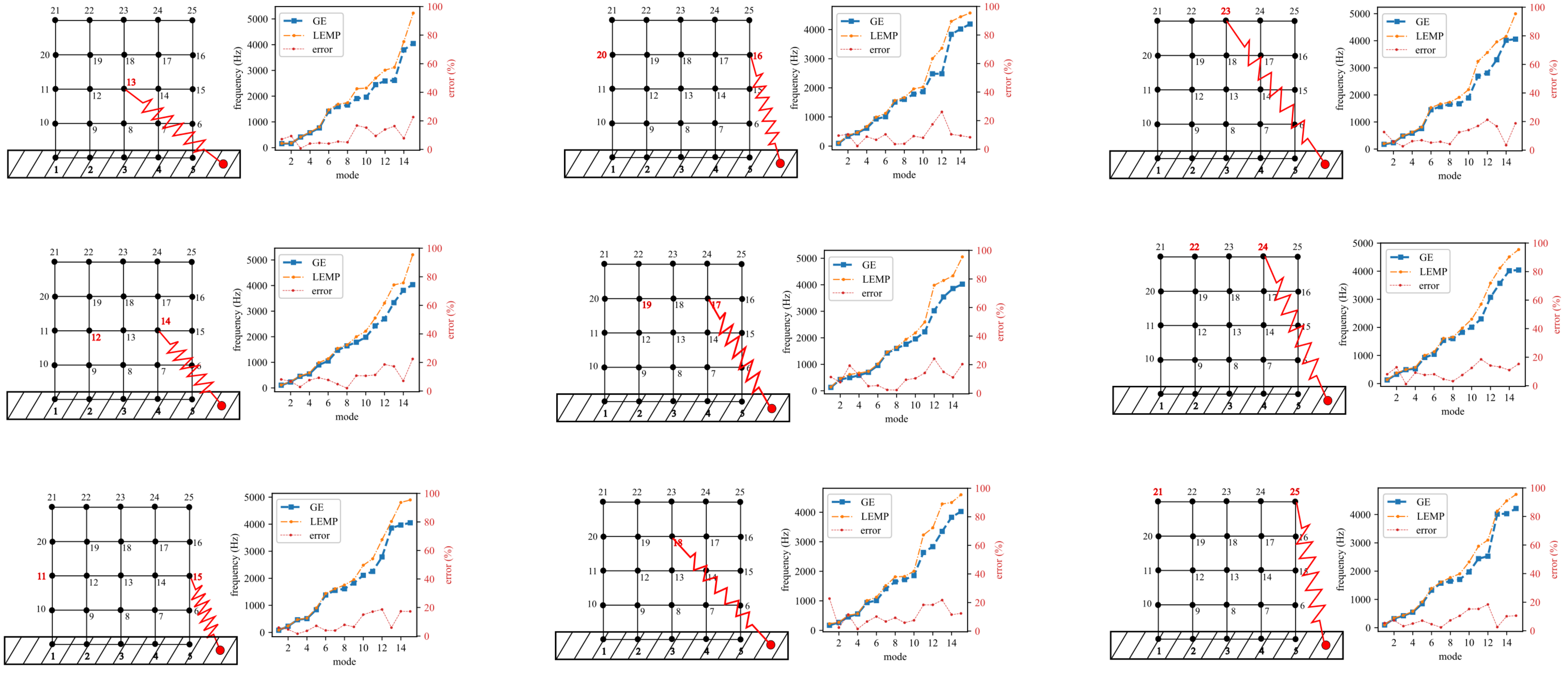

Error at nodes

	% error at nodes					% error at nodes					% error at nodes					% error at nodes					
mode	6	7	8	9	10	11	12	13	14	15	16	17	18	19	20	21	22	23	24	25	count
1	2.532117	1.987089	2.686049	2.039476	2.574719	5.890645	7.965409	7.192803	8.101189	5.912551	9.497408	11.3315	22.76656	11.47762	9.488718	5.442432	8.088518	12.67039	8.049198	5.424116	0
2	1.748493	2.466974	2.074156	2.063405	1.719738	4.619095	7.172105	9.368445	6.82218	4.638922	10.38528	7.715702	2.41712	7.677894	10.38767	7.161676	12.92952	6.074223	12.94797	7.218211	2
3	0.953186	1.316698	0.813959	1.117853	0.946491	1.622843	3.017837	0.802334	2.8354	1.606298	2.176486	19.31973	11.59083	18.66725	2.193322	3.166835	1.183541	2.701019	1.199321	3.237814	15
4	0.521762	1.485406	2.826987	1.614323	0.552273	3.596503	7.637173	4.136615	7.63092	3.629259	8.734441	12.74896	1.519571	12.62904	8.707256	5.018165	9.199682	6.276045	9.173027	5.037879	9
5	4.700076	6.679389	3.521589	6.013716	4.744664	7.170588	9.990671	4.552547	9.260694	7.141813	6.561462	4.950766	6.674359	5.247573	6.607372	7.077355	7.587955	6.927779	7.587955	7.083466	2
6	5.323287	6.451122	4.052768	6.503801	5.323287	3.910083	7.563697	4.103226	7.73393	3.9568	10.35219	5.378282	10.129	5.434294	10.38407	4.592651	8.067761	5.231131	8.051535	4.599511	2
7	0.766019	0.979711	1.636351	0.986735	0.801727	3.834675	4.717042	5.510132	4.827965	3.864438	3.524868	2.327415	6.722739	2.226873	3.543342	2.234841	4.55528	5.883271	4.655953	2.35604	17
8	0.615614	3.333333	3.5367	3.298704	0.708041	7.865297	2.171119	5.033873	1.990343	7.854778	3.76996	2.219439	9.296427	2.279138	3.821924	7.067435	3.274497	4.274147	3.215992	7.256163	11
9	7.734375	3.905734	5.084374	3.62077	7.997004	6.362704	11.00658	16.736	10.7485	6.453861	9.132671	9.428189	5.873433	9.418856	9.002907	10.38084	7.378596	12.53273	7.524065	10.44199	0
10	7.12605	3.78518	2.77063	3.562164	7.038741	15.00322	10.56295	15.25906	10.64363	14.99295	7.980973	10.4069	7.539742	10.28782	8.098754	15.11541	12.33968	14.06895	12.4735	15.21763	0
11	5.682823	10.78792	7.697923	10.6093	5.700386	17.08992	11.37399	9.440886	11.26693	17.09602	17.397	14.18785	18.35887	14.21432	17.44371	15.27005	18.39393	16.90804	18.48926	15.27005	0
12	16.41868	13.98043	16.83436	14.0326	16.50432	18.69787	18.48873	13.96	18.58958	18.63622	26.12778	24.16503	18.38648	24.10023	26.1124	18.29072	14.16208	21.24383	14.14289	18.4094	0
13	10.00126	16.19612	18.27292	16.28644	9.983127	5.86878	17.09173	16.32266	17.25441	5.889439	10.39051	14.89921	21.69847	15.00948	10.35073	2.5435	13.18581	16.70431	13.16257	2.571872	1
14	12.15216	7.737914	5.404227	7.856141	12.17155	17.33568	7.093032	7.79415	7.11567	17.34773	9.475202	11.05434	11.52126	11.05639	9.475202	10.13109	10.91125	3.439656	10.95864	10.1351	0
15	12.0695	12.4493	12.30422	12.37868	12.09239	17.03949	22.45205	22.63504	22.4595	17.26478	8.317759	20.35461	12.34558	20.46007	8.32779	10.62872	15.2532	18.76341	15.25852	10.55855	0

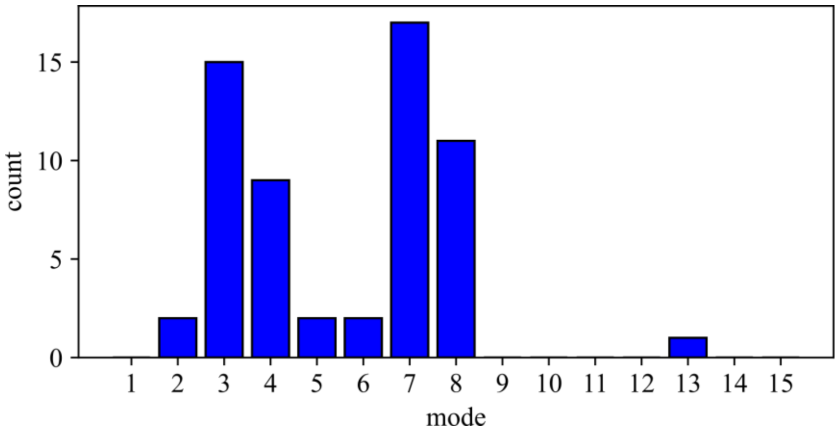

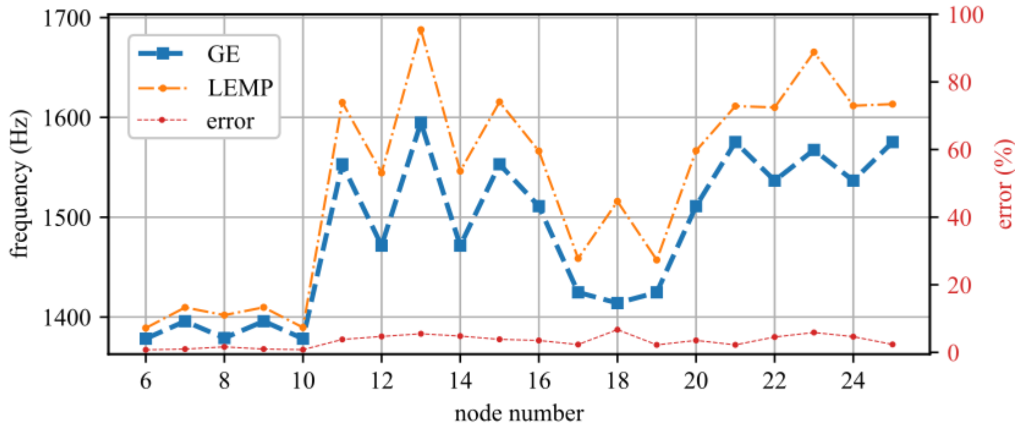

Multiple state change timing with LEMP

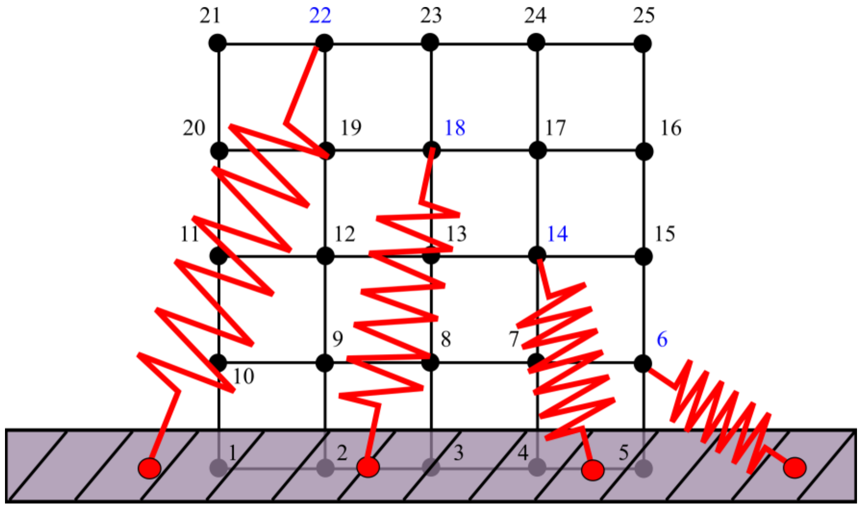

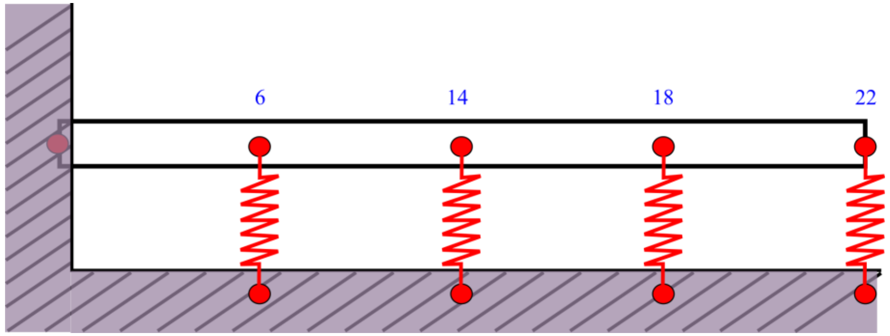

Single state change time on 25 node plate

GE	LEMP	speed
9.01 ms	0.43 ms	20 x

Four state change time on 25 node plate

GE	LEMP	speed
36.04 ms	1.62 ms	22 x

Contents

Conclusion

- Developed a real-time structural model updating framework using the Local Eigenvalue Modification Procedure (LEMP) tailored for high-rate dynamic environments.

- Achieved millisecond to microsecond-level latency in structural state estimation, significantly outperforming traditional general eigenvalue-based approach.

- Validated LEMP on both numerical simulations and experimental testbeds (DROPBEAR), demonstrating robust performance under changing boundary conditions and structural modifications.

- Extended LEMP from 1D beam systems to 2D plate structures, showcasing its versatility across domains and scales.

- Positioned LEMP as a viable tool for next-generation smart structures and edge-based monitoring systems, paving the way for future adaptive control and damage mitigation strategies.

Acknowledgement

This material is based upon work supported by the Air Force Office of Scientific Research (AFOSR) through award no. FA9550-21-1-0083. This work is also partly supported by the National Science Foundation Grant numbers 1850012 and 1956071. The support of these agencies is gratefully acknowledged. Any opinions, findings, conclusions, or recommendations expressed in this material are those of the authors, and they do not necessarily reflect the views of the National Science Foundation or the United States Air Force.

THANK YOU!

Questions or Comments?

Emmanuel A. Ogunniyi
Ph.D candidate, Mech Engr.
ogunniyi@email.sc.edu

UofSC South Carolina